Author's Response

for the second review of

"**Four decades of Antarctic surface elevation changes from multi-mission satellite altimetry**"

We are grateful for the constructive and helpful comments of both referees and the editor himself. We think that the very specific hints helped to significantly clarify the manuscript in the description of the methods, the results and in the interpretation as well. We have rearranged some sections, also between the supplement and the main part, and think that now, the text reads more fluidly. The description of several additional data sets, as the validation data sets, the FDM, the firn density grid, the SMB and GRACE has been clarified.

On the following pages, we respond to all referee reports in detail, followed by a version of the manuscript containing all changes made since the reviewed version.

Authors response to referee report #1

General comments

• *Combining laser altimetry estimates with radar altimetry estimates is a non-trivial task (e.g. Fricker and Padman, 2012). Not simply due to the differences in footprint diameter but by potentially measuring different surfaces. The comparisons with NASA Operation IceBridge in West Antarctica and the Peninsula are helpful for this but it was difficult to discern the local discrepancies between the measurements as presented.*

Besides the different topography sampling, we agree that also the firn penetration is a challenge in this combination of different techniques. This penetration might even vary in time as the surface properties of the upper firn layers change, e.g. due to the depositioning of fresh snow. Such temporal variations in the penetration depth of the radar signal, however, are significantly reduced by our low threshold retracking as it reduces the overall influence of snowpack penetration. The remaining effect of changes in firn properties is accounted for by our backscatter correction. Hence, we consider the remaining penetration bias of radar altimetry w.r.t. the surface as invariant in time. This constant bias between radar and laser is removed as we reduce each technique's time series by their respective elevation at the reference epoch 09/2010. This reduces any constant offset between the time series, may it be due to the topography sampling, the firn penetration or remaining calibration issues.

We added these points to Sect. 3.2 and 3.3.2 to make the reader more aware of the fact that besides the spatial sampling also other factors may be responsible for these biases. Nevertheless, any constant biases between the time series, may they originate from instrumental calibration, sampling issues or firn penetration, are removed in this step. Concerning the validation with ICEBridge, we added some more detailed plots to the supplement as indicated in the line-by-line comment to highlight the level of agreements as well as the noise on smaller scales.

• *The paper can be still be difficult to follow at times. The manuscript could be reorganized and restructured to not repeat information between sections.*

We changed the order of Figs. 9 and 10 and the related discussions. This also helped to eliminate some repetitions there. Furthermore, we removed the former Sect. 6.1 and integrated the most important content elsewhere. We hope that these and the other changes helped to make it easier to follow now.

• *The data and methods sections could also still be more detailed. Are the GRACE basin time series results simply an available product? If so, it could include a citation for the data repository. If not, should detail the GRACE processing scheme as you start to diagnose specific uncertainties in time-variable gravity measurements.*

We used the GRACE product of the Antarctic Ice Sheet CCI project. This information and links to the data repositories has been added.

Line-by-line comments

Abstract This is much improved from the previous versions.

Good to hear.

P1, L14–15 I would cite Shepherd et al. (2012) as a reference the time-variability of Antarctic surface elevation change.

Done.

P2, L9 Remove "Also" from the start of this sentence.

Done.

P2, L18 "Finally, we merge all time series from both radar and laser altimetry"

Changed.

P2, L22 What do you mean by "three-month temporal averages sampled every month"? A moving average of the elevation data with a three month sliding window?

Exactly. Changed the sentence to make this more clear.

P2, L24 "independent in-situ and airborne datasets, satellite gravimetry estimates, and regional climate model outputs".

Done.

P2, L25 I wouldn't use SEC as an acronym here and elsewhere
In contrast to dh/dt, which describes the rate of surface elevation change, the surface elevation change "SEC" explains our result very well: the elevation change w.r.t a reference epoch. We cannot see any reason why this acronym shouldn't be used.

P2, L26–27 I would phrase it something like "The recent elevation changes of Pine Island Glacier in West Antarctica, Totten Glacier in East Antarctica, and Shirase Glacier of Dronning Maud Land in East Antarctica are put in context with the extended time series from radar altimetry"
Done.

P2, L30–31 I would remove these two sentences ("While this paper. . . ").
Done.

P3, L3–4 I would place the release numbers of each dataset in the main text.
Modified accordingly.

P3, L8 Should at least include citations for the pre-processing steps used to remove corrupted ICESat returns within this section.
The outlier screening is an important step, but we think that if we would present more details concerning ICESat here, the reader would wonder why no details concerning the other missions are presented here. Instead, in order to keep the main text short we refer to the supplement, where all these technical details for each mission can be found.

P3, L14–20 Were the ocean and ice modes both used everywhere or was the ocean mode used only in the interior plateau? If different regions were used, a map would be beneficial.
We did not employ any regional selection. If the data screening and flags indicates a measurement as "valid", it is used. However, there is also an iterative outlier screening in the repeat altimetry processing. The spatial distribution of the data can already be seen in Fig. S3.

P4, L4–6 Could include detail on the advantages and disadvantages of the "relocation" and "direct" methods. Is the "relocation" method valid over the entire timespan of measurements? The ice sheet has changed surface shape over this time period and a single DEM, particularly one from the latter period of observations, may not be accurate.
The text has been modified accordingly. Concerning the temporal changes in the DEM, we would like to mention that for the POCA, only the relative topography within the BLF is relevant. For regions, that are observable by radar altimetry (i.e. flat enough) we do not expect a significant effect of changes in the relative topography within the BLF on the location of the POCA.

P4, L11–12 Is this sentence about optimization necessary? Could simply state the differences from prior work.
We think it is necessary as the original method of Roemer et al. (2007) is more precise, while we use a simplification. For each shot, the DEM-to-satellite distances are calculated for every cell within the beam limited footprint (BLF). After that, Roemer et al. (2007) used a 2x2km moving window to find the closest average pulse limited footprint location. Instead, we do not use this moving window but smooth the DEM instead. This saves a lot of computational time, compared to calculating all the moving averages for each shot in each BLF again. We modified the text to make this difference more clear.

P4, L12–13 Will there always be a unique determination of the POCA location with this methodology?
Surely, cases might exist where two local maxima might have exactly the same distance to the sensor. However, in such a case, the other techniques would not correctly handle this situation as well. Instead, they would use some "mean" slope, which is just a trade off and would in fact assign the measurement to somewhere completely different. Instead, this approach would refer the measurement to one of the two maxima, which is definitely the preferred method.

P5, L1–8 This is a good review of the effects of spatial aliasing. However, the penetration of the radar signal into the surface is another bias term that would potentially affect rate estimates. Could add a caveat.

For this reason, Lake Vostok is a great spot to study penetration effects in the absence of topographic features (see Schröder et al., 2017). The text has been modified accordingly .

P7, L9–11 At least for laser altimetry, 1km may be too coarse of resolution for the assumption of planar surfaces in coastal regions (Markus et al., 2017). Could include additional higher order surface shape terms.
This might be true for several cases. This point has already been discussed later in Sect. 6.3 with regard to the APIS. However, we prefer to fit as few parameters as possible for the sake of robustness. As discussed by Ewert et al. (2012, Fig. 2d), an unfortunate distribution of tracks within the repeat track box might lead to large ambiguities between elevation differences due to topography and due to real elevation changes. This becomes even more critical as more parameters are fitted.

P9, L1–2 Rewrite to something similar to "Over regions of flat topography, such as the interior of East Antarctica, the weights between PLRA and ICESat are comparable".
Done.

P10, L6 The use of FDM is an interesting approach. I would add the caveat that changes in ice dynamics would not be captured by this metric.
Done.

P11, L5–10 Is applying a uniform single bias just forcing the linearity condition to regions where it might not be viable? The distributions of biases in the supplementary material appears to be not random but fairly spatially correlated.
The linearity condition only selects the regions which are proven to be very likely linear. From these regions, we calculate the average bias. In any other region, where we assume a non-linear signal, the bias does not force the data sets to become linear. It just corrects for the most likely bias, observed over other regions which are close to linearity.

We are aware of the fact that the spatial pattern of this bias is a big issue in the calibration of Seasat and Geosat. Therefore, we use the significantly larger standard deviation of 85cm for Seasat and 61cm for Geosat in our error propagation everywhere, instead of the much lower values for the other missions in Fig.S4. However, as we do not fully understand the origins of these patterns, we do not want to extrapolate the spatial pattern to the coastal data.

P11, L24 These instruments could be detecting different surfaces beyond the topographic sampling discrepancy.
Text edited, see first bullet of the general comments.

P12, L1–2 Could possibly use an interpolation scheme with tension or inherent smoothing.
We decided against an interpolation scheme with tension in order to avoid extrapolating values to regions where no real measurements exist. Instead, we limited our smoothing to regions within a footprint, hence to the measured locations only. This is already discussed in Sect. 3.3.3 and in Sect. 6.3 with regard to the APIS.

Figure 7 Difficult to discerns the differences from GNSS and Operation IceBridge with these maps. Lots of dots area overlapping. Is the color scale in a) and d) the same as in b) and e)?
We added some more detailed maps of key regions in the supplement (Fig. S6). A comment concerning the color scale has been added as well.

P14, L2–3 Could add possible explanations of the difference between the airborne altimetry measurements and the combined estimate.
Done.

P14, L4–8 Could expand to note the potential error sources between GNSS and altimetry. This seems like a fairly large amount of variability for East Antarctica. Could potentially use other datasets for validation as well.
Explanations for potential error sources have been added. We compared our results to elevation changes from OIB, kinematic GNSS and (as a correlation coefficient) to the FDM. We conclude the section with a statement about the issue that we could not validate the earlier data due to the lack of appropriate validation data sets.

P14, L10 Remove "we have to stress that"
Done.

P14, L12 I would change it to "publicly available" versus "available to us".
Done.

P14, L15–17 Remove "Before we can compare this model to our SEC results, however, it is important to mention that"
Done.

Figure 8 The RMS with the FDM seems surprisingly high.
This RMS did not mean an error, it is the squared mean of the anomalies. Figure 8b should give an impression where we can expect a (non-linear) signal above the noise level of the altimetry, hence, where we can expect a correlation at all. We changed the label to make this more clear and modified the text as well.

P16, L3 In terms of spatial resolution?
"temporal" added.

P17, L15 "rates within uncertainties and very close to zero"
Changed.

L17, L17–22 The discrepancy with Zwally et al. (2015) is an important finding.
We think so too, however, this has already been discussed several times, e.g. by Scambos and Shuman (2016), Richter et al. (2016) or at different points in Schröder et al. (2017).

Figure 10 Would the early mission data over the Antarctic Peninsula be at all viable? The Peninsula is particularly difficult to measure with radar altimetry (Shepherd et al., 2012).
In Sect. 6.1, we discuss that the APIS is one of the regions where the early data is very noisy due to difficult topography. This is the reason why we do not calculate a basin mass trend here (see footnote for Tab. 2).

P17, L31–P18, L4 This paragraph repeats a lot of information provided previously about individual glaciers. Could be merged.
The presentation of the results at Fig. 9 and Fig. 10 have been switched and in this context, also some repetitions have been eliminated. We think that this makes the whole results section now easier to follow as we now first give a general overview before we discuss the details.

P17, L 34 Remove "too"
Done.

P19, L7 "The surface elevation time series is converted into ice mass changes in order to determine their effect on global sea level."
Edited.

P19, L7–8 "The elevation time series are corrected for uplift rates related to glacial isostatic adjustment (GIA) using coefficients from the IJ05_R2 model (Ivins et al., 2013)."
Edited.

P19, L9–10 The elastic effects would likely be much more localized than the outputs from a GIA model, and would be related to the modern-day change rather than the unloading since the LGM.
We agree that the formulation was misleading here. The scaling factor is applied to the SEC time series, not to the GIA model. We edited this sentence to make this more clear.

Figure 11,12 As the area of observation changes with time, would it be more appropriate to calculate the average surface mass density (kg/m 2) change rather than the total mass change of these sectors (i.e. divide the resultant mass by the total area)?
As the elevation changes are not uniformly distributed in a basin, we think that such an average surface mass density would have the same issues. As the largest changes typically occur in difficult terrain for radar altimetry, an observational gap in an area with large changes would also significantly affect an average mass density. However, for most of the basins, there are no significant changes in the observed area.

P21, L7–8 "We integrate our measurements over larger regions to calculate the cumulative mass anomalies for individual drainage basins and major Antarctic sectors (AIS, WAIS, EAIS, APIS). Our basin delineations are from Rignot et al. (2011a), which have been updated for the second Ice Sheet Mass Balance Inter-comparison Exercise (IMBIE-2, Shepherd et al., 2018)."
Changed.

Table 2 Is the area of observation constant for these volume rates?
The rates were obtained from epoch differences of the time series and the observed area in Tab. 2 refers to the minimum area of any of those epochs. For the <81.5°S sector, they refer to the time series displayed in Fig. 11. We agree that it causes an issue if the area is not the same at both epochs, however, as it can be seem from Fig.11, significant differences in the observed area occur only at the APIS. To account for the errors which might be imposed by unobserved areas, we apply an estimate for the magnitude of the effect to the uncertainty as explained in the supplement at F.2.

P22, L7–9 Same GIA model outputs used to correct the GRACE data?
Yes. More details concerning the GRACE data have been added to the manuscript as described at bullet 3 of the general comments.

P11, L4 What is the reference period used to calculate SMB anomalies? 1979–2017?
We are not sure to which exact location this comment refers. However, we added the modeled period (1979-2016, which is the same as for the FDM) to the text in Sect. 5.2 once more.

P22, L17 Variations and attribution of Cp-D mass change shown here are supported by Velicogna et al. (2014) and Li et al. (2016).
Good hint, we added the references.

P22, L18–19 "There is less agreement in regions where surface mass balance change may not be dominant, such as of the Getz and Abbot regions (F-G) in West Antarctica."
We modified the passage but we would like to stress the different components of the signal more. In the short term variations, all data sets agree, while only the long term changes are not contained in the SMB model, hence we attribute them to ice dynamics.

P22, L20–21 I'd suggest something like "In some regions, there are also significant discrepancies between the different atlimetry and GRACE data sets. These differences can be due to inadequate sampling by radar altimetry, such as in the northern tip of the Antarctic Peninsula where steep regional topography and small outlet glacier size limits the recovery, leakage in the GRACE estimate between different sectors, and uncertainties in the individual measurements and geophysical corrections."
The passage has been modified accordingly.

P22, L34–35 Could add that some of the disagreement with Shepherd et al. (2018) is due to differences in the estimates for the Antarctic Peninsula where retrieving reliable radar altimetry estimates is non-trivial
Done.

P23, L17 "better than a centimeter per year in some regions". This wouldn't be expected in some coastal and mountainous regions as you explain in the following sentences.
This phrase has been modified.

P24, L8 "Over 25% of the ice sheet, largely in the coastal regions of East Antarctica, the time series can be extended back 40 years."
Changed.

P24, L8–9 Could reference ? to indicate that the period of observation for single instruments is short compared to climatic oscillations. Having the extended time series helps separate elevation change due to climate variations, with potential accelerating volume losses.
Very good point. We added this argument.

P24, L13–14 Remove "e.g. at point A in Fig.9c of 0.55 ± 0.50 m with the change modeled using the FDM (0.48m between 2008 and 2012)". It makes the sentence hard to read.
Put this to a separate sentence to make it easier to read.

P25, L8–9 Alternatively it means the altimetry measurements are sensitive to variations in low density material, such as changes in accumulation.
They are sensitive to variations in low density materials as in high density materials as well. The point here is that we want to explain, why the ice dynamic changes (as in the Amundsen Sea basins) show up in darker red in the GRACE mass time series in comparison to altimetry, while the mass gains in DML are less pronounced.

P26, L1–9 This section about radar altimetry in the Peninsula is important as it provides context for the results.
Great, thanks.

P26, L22–23 "Part of the discrepancy with the GRACE results could be due to uncertainties in the geophysical corrections applied, such as the effects of glacial isostatic adjustment. More work, similar to the Ice Sheet Mass Balance Inter-comparison Exercises, could help identify the key processes leading to the disagreement."
Changed accordingly.

P26, L27–29 "We showed that the methods used here improved the overall precision by 50% over the standard datasets available from ESA and NASA."
Done.

P26, L29–31 Mention the comparison with airborne altimetry.
Done.

P27, L1 "Observations from the Seasat and Geosat missions extend the time series in the coastal regions of East Antarctica back to 1978."
Done.

P27, L13 "might be explained by the density mask used or uncertainties in the GRACE processing"
Done.

P27, L16–18 I would use something like "We believe that our multi-mission combination approach can provide an important tool for including and providing context for the ICESat-2 data with observations spanning the past few decades."
Modified accordingly.

Supplement What is the reference frame of each of these datasets? What ITRF was used for the final combined product?
All missions referred to WGS84, except ICESat, which originally refers to a T/P ellipsoid. However, also ICESat data come with corrections for WGS84, which were applied as mentioned in A.4. We stated more clearly now that all other missions already refer to WGS84. The final product does not contain absolute elevations, only elevation changes, hence, it does not refer to any ellipsoid.

References

Ewert, H., Groh, A., and Dietrich, R.: Volume and mass changes of the Greenland ice sheet inferred from ICESat and GRACE, J. Geodyn., 59–60, 111–123, https://doi.org/10.1016/j.jog.2011.06.003, 2012.

Richter, A., Horwath, M., and Dietrich, R.: Comment on Zwally and others (2015)-Mass gains of the Antarctic ice sheet exceed losses, J. Glac., 62, 604–606, https://doi.org/10.1017/jog.2016.60, 2016.

Roemer, S., Legrésy, B., Horwath, M., and Dietrich, R.: Refined analysis of radar altimetry data applied to the region of the subglacial Lake Vostok / Antarctica, Remote Sens. Environ., 106, 269–284, https://doi.org/10.1016/j.rse.2006.02.026, 2007.

Scambos, T. and Shuman, C.: Comment on 'Mass gains of the Antarctic ice sheet exceed losses' by H. J. Zwally and others, J. Glac., 62, 599–603, https://doi.org/10.1017/jog.2016.59, 2016.

Schröder, L., Richter, A., Fedorov, D., Eberlein, L., Brovkov, E., Popov, S., Knöfel, C., Horwath, M., Dietrich, R., Matveev, A., Scheinert, M., and Lukin, V.: Validation of satellite altimetry by kinematic GNSS in central East Antarctica, The Cryosphere, 11, 1111–1130, https://doi.org/10.5194/tc-11-1111-2017, 2017.

Authors response to referee report #2

The manuscript has improved significantly due to the changes addressing the issues raised by the reviewers and posted comments.

The main goal of the manuscript is to introduce a new method for deriving multi-mission elevation changes and mass change time series of altimetry data. The new results are used for investigating climate and ice dynamics related changes of the Antarctic Ice Sheets.
Part of the methodology is described in the supplementary information and some of the arguments of selecting certain models, eg., planar surface fit vs. higher order polynomial, are also explained in the supplement only. The supplement is well written and it is easy to follow. However, the main manuscript is fragmented and unclear in some places, making it difficult to follow the discussion as it moves from the main paper to the supplement and back. The manuscript should explain all main points of the study indicating where the reader should consult the supplement and references for details.
The intention of this separation was to keep the (already quite long) document short by providing only the main points in the manuscript while providing more details (as the calculation of the uncertainties or several maps for each mission) for the interested reader in the supplement. However, we agree that the choice of repeat altimetry parameters is too important to appear in the supplement only. Therefor, the former Section C.1 has now been completely integrated into the main manuscript.
In section 3.3, we changed the reference to the supplement instead. We believe that it will be very hard for a reader to follow the main idea if we discuss all the details of each merging step as the processing parameters, outlier checks and the specific arguments for these decisions in the main part.

Also, the grammar needs some improvement. For example, the words respective or respectively are used a total of more than 60 times (paper and supplement), in my view, often unnecessarily.
We agree and eliminated or replaced many occurrences of this word. Many other changes have been made with regard to all detailed comments.

Following recommendations from the review of the original manuscript, the authors included a conversion of the elevation changes to mass changes. The applied method uses an ice density mask defined by a priori knowledge of the spatial distribution of changes due to ice dynamics and surface processes for the conversion. To my best knowledge, this technique has not been used before for long periods with significant changes in ice dynamics. There is ample evidence of changing Antarctic ice dynamics in the literature and in the manuscript itself. The authors describe the technique as "straightforward and robust", but they don't provide any assessment of its performance. Considering the changes in ice dynamics and the complex variations of firn-compaction and density during the 40 years spanned by the altimetry record, I expect large errors. These errors, only partially accounted in the error budget, could be responsible for some of the significant discrepancies between the mass balance derived from GRACE and altimetry in the study.
We agree that ice dynamic processes might also be involved in other regions as indicated by the density mask. This is discussed as a likely cause for the mentioned discrepancy between altimetry and GRACE in Sect. 6.3. At least for some of the regions, the preferred density should be chosen according to the combination of ice dynamics and surface processes. Zwally et al. (2015) discuss, that such a pseudo-density could even be out of the range between firn and ice density if both processes have opposite signs. This is clearly a caveat of this approach. However, without additional information, the selection of a more appropriate density is not possible. Such a detailed analysis is far beyond the scope of this paper. Instead, the main intention of the mass time series here was to make the altimetry data comparable to alternative data sets of mass changes as SMB or GRACE. This comparison can, in fact, be interpreted as the assessment recommended. If the FDM/SMB data sets were already used in the volume to mass conversion, such a comparison would not be possible.

Also, the manuscript and the references do not describe the method with sufficient details. Was the density an average density for a given time period? What was this time period and how did the authors account for the different length of the altimetry record?

This surface density grid is described in Ligtenberg et al. (2011) (see also Fig.7A therein). It is also publicly available via the Quantarctica (http://quantarctica.npolar.no/) data collection. The surface density (taken to be the density of the upper meter) is assumed to be constant over longer times, which is almost always done. In the IMAU-FDM, the surface density is parameterised using the long-term climate: temperature, accumulation, and wind speed.
The passage has been edited to add some details for clarification.

Was the firn-compaction removed?
We did not remove a firn compaction as this effect affects mainly short time scales. Over long time scales, which is the main scope of this paper, only a persistent instability in atmospheric conditions would cause an effect of firn compaction. Such an instability, however, wouldn't be detectable even by firn modelling due to the steady-state condition (see next answer).
We added this discussion to Sect. F.2.
Also, the manuscript several times states that the FDM and SMB time series do not contain long-term changes. This is only partially true. Both FDM and SMB assumes a balance period. The inadequate knowledge or lack of such a balance period could result in an error in the FDM and SMB anomaly trends, but the remaining components of the long-term change will be correctly reconstructed. The cumulative SMB anomalies presented in the manuscript show several examples of these long-term trends (e.g., Fig 13).
Here, we have to contradict respectfully. For the IMAU-FDM we use, the steady-state assumption is a precondition as described in Ligtenberg et al. (2011). It presumes no overall trend over the modeled period (1979-2016 in this case).
The SMB from RACMO2 does not presume a steady-state. It does not assume a balance period either. RACMO2, the regional climate model, is forced at the lateral boundaries and the atmosphere within the domain is allowed to evolve freely. The simulated weather (and subsequent SMB) is therefore not influenced by any balance assumption. However, in order to get an ice sheet mass balance, this SMB needs to be combined with ice discharge (see e.g. Rignot et al., 2011). As we do not have accurate ice discharge data, which would introduce additional sources of error, we focus on the anomalies in SMB during our comparison. As we reduced the mean rate of each cell, each of the cumulated SMB anomaly curves start and end at the same value. These values may be different from zero as the curve has been adjusted to zero at 09/2010, however, there is no trend.

Nevertheless, we agree that we maybe did not explicitly enough explain that we use SMB anomalies. Therefore, we modified the introduction of this data set to be more precise and introduced the abbreviation SMBA.

Detailed comments:
Page 7. Figure 3. This figure is only referred after the reference to Figure 4. Either the figures order should be changed, or a reference to this figure should be included.
We agree and moved the Figure to Sect. 3.3.

Page 9, line 8: I assume that all other corrections were performed and not "omitted"
The parameters of topography slope and backscatter regression are omitted in the recombination, which has the effect that the resulting time series can be considered "corrected for these effects". We changed the formulation making it more clear hopefully.

Page 9, lines 8-14: I can only guess the meaning of "These "res" [residuals] represent the anomalies of typically a single satellite pass towards all respective parameters including the linear rate of elevation change." It needs to be rephrased.
We agree and added the information about typical repeat cycle periods, which needs to be known to understand this statement.

Page 11, lines 27-28. As it has been documented, significant changes occurred in ice dynamic during the 8 years used for the correction (e.g., Flament and Remy, 2012). The density of sampling would probably allow using a quadratic approximation to allow for non-linear dynamics. What was the reason for using the linear approximation and what could be the impact of the modeling error?
This is true for cells where e.g. Envisat and CryoSat observations cover the whole time period. However, we have to consider that there may be also cells where only ICESat observations are available, which sample only some of the months during the laser campaings until 10/2009. Here, an extrapolation including a quadratic term might lead to large errors.

3.3.3 Merging different techniques: A region with a 30 km diameter is large enough to exhibit variations in thickness change rates. Therefore, as the authors have stated, the residuals of the elevation changes within the region could reflect not only measurement errors but real variations. In my opinion, using a formal error propagation through the entire error assessment, i.e., instead of including equation (4) in Supplement C.4 could provide a better error estimate.

We agree about the variations within this radius but please consider also, that we used a Gaussian weighting, which has the effect, that a value at 30km distance would have only 0.12% of the weight of a comparable value at the center.

We agree also that equation (4) in C.4 is just a simplification of a full formal error propagation of this averaging, as covariances are not included in the first term. Instead, we added the second term to account for such effects. For a full error propagation, a full variance-covariance matrix would be necessary, including the spatial correlation of the inter-mission offsets. Such correlations would need to be calculated when different missions are combined. However, this combination is a stepwise approach which means that the uncertainties of the combination of the overlapping and non-overlapping missions would first need to be propagated to the combined PLRA time series. After this, another error propagation with a full variance-covariance matrix would be necessary for the combination of the techniques. As in fact, for Seasat and Geosat all measurements are correlated due to the average offset correction, a full variance-covariance matrix would have the dimension of $n \times n$ where n is the amount of all 1km grid cells (ca. 23.000.000). Furthermore, due to the temporal averaging of the PLRA offsets and the time period in the fit of the technique offsets, these dimensions have to be multiplied by the number of months included. Such a matrix is needed for EACH cell for a formally correct error propagation. Handling such a system of matrices is not possible with the computational resources we have. Besides these points, also such a full model of error propagation would still be incomplete as further correlations, e.g. between consecutive cells which are observed by the same satellite orbits would not be accounted for here. To overcome all these problems, we add the second term in Eq. (4), which we consider as an conservative simplified estimate for these effects.

Page 12, line 9: What is the meaning of the "flow line of outlet glaciers"? Regions of fast-flowing outlet glaciers? Measurements along the flowlines of fast-flowing outlet glaciers?

Changed to fast-flowing outlet glaciers.

Page 12: showing annual rates rather than differences relative to the reference time would make it easier to interpret the changes. Otherwise, the sign of the relative anomalies is different for dates preceding the reference dates and those after the reference data. Also, using differences relative to the reference time results in a scaling of the variation of elevation differences within the averaging area, as mentioned in the manuscript, and makes the interpretation of the error difficult.

We take this comment serious as it has been raised more than once. Nevertheless, we think it is important to show our resulting grids as they are (elevation differences w.r.t a reference epoch and their uncertainties) because this is important to understand the characteristics of the products derived from these grids. This accounts e.g. to the understanding of the standard deviations related to these absolute SECs during the smoothing, the spatial distribution of linear rates over different intervals, or errors related to these rates. Elevation change rates as suggested here can already be found later in the results section (Fig. 9 now)

Page 12, line 10: I suggest to refer to the area of averaging, rather than to the area of smoothing.

Changed to "weighted averaging" as we agree that this is more precise but want to make the reader also aware of the fact, that we used weights. Hence, as discussed before, differences on the very edge of the area of averaging have only very small weights and hence also low influences on the results.

4.1 In situ observations. Briefly describe the measurement type and processing method for both types of observations (e.g., ground GNSS traverse using snowmobile, or airborne laser altimetry). Include the error of the in situ measurements based on literature. Elaborate on the reason of the difference between in situ measurements and new results in the flat interior region.

Changes have been made accordingly.

4.2 Firn model. Include details of the particular FDM use. Did it assume the same steady state period as in Ligtenberg et al., 2011? What was the temporal and spatial resolution? How were the

modeled FDM changes interpolated to the altimetry grid? Finally, what is the error of the FDM model?
Details concerning the FDM resolution have been added. We agree that also the interpolation to the altimetry grid is one of the steps which has to be done. As our altimetry (10x10km) has a significantly higher resolution as the FDM (27x27km), errors due to this reprojection can be neglected. This is simply a technical detail and has no influence on the results.
Sensitivity simulations of the FDM show linear relations between a %-change in accumulation and snowmelt (the governing climate processes of firn layer variations), which can be used to quantify the uncertainty of the FDM. However, alternatively, a validation with observations can also provide information on the influence of potentially unmodeled effects. Hence, a cross-validation as performed here provides independent uncertainty estimates.

It is difficult to understand the comparison method applied between the FDM and the altimetry records. A figure, illustrating the approach would be very useful.
We added such a figure to the supplement.

Detailed question: Were both time series detrended independently using linear approximations? In page 14, line 24: "RMS of these anomalies from the altimetry data", while in the figure caption for Fig. 8. b): "RMS of the detrended anomalies of the 1992-2016 altimetry time series". Do you refer to the same RMS in both places? Is it the RMS of the difference between the detrended FDM and detrended altimetry time series computed for each grid cell? Why is the RMS reflect "the magnitude of seasonal and interannual variations"? I assume that both the detrended FDM and the detrended monthly altimetry data reflect seasonal and interannual variations, so the RMS of their difference would be related to the errors and sampling of the two data sets and any short-term variations in ice dynamics.
Each of the time series was detrended using a trend fit to the respective time series. We replaced the term RMS as it seems to cause confusion here. RMS is simply the description of the method used to calculate the average amplitude of the non-linear signal. In Fig. 8b, the RMS means the root of the mean squared detrended SEC from altimetry. We clarified this in the captions and the text. We agree, that this represents not only interannual but also seasonal changes and added this to the text as well.

Figure 8. Capital letters and drainage basins in a) are not explained and used in this section. The point density needs a color bar.
Figure modified accordingly.

Results, 5.1 Surface elevation changes
Table S2. Include the projection system used for the X, Y coordinates and latitude, longitude locations. Expressing the multiyear changes as annual change rates would make it easier to interpret the results, e.g., relative elevation at a later date minus relative elevation at an earlier data divided by the number of years would always give negative values for thinning rates and the normalization would allow a direct comparison of the change rates during different time periods.
Coordinate system information added. We think, for an interpretation, the reader should refer to the plot (Fig. 10 now). These numbers in the supplement are provided as a reference for the rates in the text. Presenting absolute values of SEC here enables the reader to calculate a rates over any given interval.

Page 15, line 19: elaborate on the connection between the stable grounding line position and observed elevation changes.
Done.

Figure 9. Since elevation changes are shown as relative values, a "floating" elevation change scale would work better than the current vertical axis. What is the difference between the black and colored line in the elevation change time series?
We are not sure what is meant by a "floating" elevation change scale. We added the explanation that the black bars represents the uncertainty.

Page 16, line 3: how much longer are the new time series? Clearly articulate on the new findings that are allowed by the extended time period.
The additional time interval covered depends on the data used in the respective studies. While

Pritchard et al. (2009) or Flament and Rémy (2012) use only one mission, Zwally et al. (2015) processed results for different missions. However, the advantage of our time series is the long-term consistency and the temporal resolution, as mentioned in the text. The following sentences clearly describe the new findings. On the one hand, these are elevation change rates from 40 years instead of a decade. On the other hand, it is the monthly resolution, which sets the rates reported by other authors and the variations as observed previously e.g. by Li et al. (2016) in a 40 year context. We modified the text to express this point even more.

Page 17, lines 8-13: it is somewhat unclear if this paragraph discusses one event (resulted from two accumulation anomalies) or two distinct elevation increases (in line 10: these event – should be either this event or these events). Also, some of the time series show a continuous increase, while others show two periods of rapid surface elevation increase. This is a nice result, and an enlargement of the figure with a more detailed description would be helpful.
We edited several parts of this paragraph and think it is much clearer now. We agree that for the points further inland, both events are hard to separate. The spatio-temporal pattern of these events in the altimetry and the FDM could help to understand the reasons, but this would require a detailed analysis. We think that such an analysis should be done very carefully and, hence, this should be done in a separate study. We hope that we can contribute to a deeper understanding with our data set.

Page 17, line 23-30: I don't understand the computation as described here.
We edited the description to make it easier to understand.

Figure 10. Show the locations of the enlargements in Figure 9 to connect the two parts of the section.
Done.

Page 18, line 9: this part should be better connected to the changes presented on the Shirase Glacier earlier in this section.
This was accounted for during the reorganisation of the content of this section.

Page 19, line 2: how much was the "huge" increase? Add a number!
Obsolete in the revised version. Numbers are included in the discussion of the time series examples here (Fig. 10c now).

Page 19, line 4: be more specific about the other regions.
Obsolete in the revised version.

5.2 Ice sheet mass time series: See general remarks at the beginning of this review.
And so refer to the answer given there as well.

6.1 Multi-mission SEC time series
Page 23, line 9: use bias instead of offset to describe the difference between change derived from altimetry data and validation data
Done.

Page 23, lines 11-13: the >0.5 correlation values do not mean that "both time series agree very well". It just means that the seasonal and interannual variations of the two time-series correlate well.
We agree and edited the formulation.

Page 23, lines 14-17: the good agreement between the detrended time series cannot establish the absolute accuracy of the SEC, especially not in a level of a few cm/yr.
We modified this to less absolute statements (which clearly depend on very regional conditions).

Page 24, lines 1-2: These sentences appear to be incomplete: "This due to the mountain ranges just north of 72°S, which lead to many losses of lock of the measurements all the way across this part of the ice sheet. The same applies to the measurements at the APIS."
Section modified.

References

Flament, T. and Rémy, F.: Dynamic thinning of Antarctic glaciers from along-track repeat radar altimetry, J. Glac., 58, 830–840, 2012.

Li, X., Rignot, E., Mouginot, J., and Scheuchl, B.: Ice flow dynamics and mass loss of Totten Glacier, East Antarctica, from 1989 to 2015, Geophys. Res. Lett., 43, 6366–6373, https://doi.org/10.1002/2016GL069173, 2016.

Ligtenberg, S., Helsen, M., and van den Broeke, M.: An improved semi-empirical model for the densification of Antarctic firn, The Cryosphere, 5, 809–819, https://doi.org/10.5194/tc-5-809-2011, 2011.

Pritchard, H., Arthern, R., Vaughan, D., and Edwards, L.: Extensive dynamic thinning on the margins of the Greenland and Antarctic ice sheets, Nature, 461, 971–975, https://doi.org/10.1038/nature08471, 2009.

Rignot, E., Velicogna, I., van den Broeke, M., Monaghan, A., and Lenaerts, J.: Acceleration of the contribution of the Greenland and Antarctic ice sheets to sea level rise, Geophys. Res. Lett., 38, L05 503, https://doi.org/10.1029/2011GL046583, 2011.

Zwally, H., Li, J., Robbins, J., Saba, J., Yi, D., and Brenner, A.: Mass gains of the Antarctic ice sheet exceed losses, J. Glac., 61, 1019–1936, 2015.

Four decades of Antarctic surface elevation changes from multi-mission satellite altimetry

Ludwig Schröder[1,2], Martin Horwath[1], Reinhard Dietrich[1], Veit Helm[2], Michiel R. van den Broeke[3], and Stefan R. M. Ligtenberg[3]

[1]Technische Universität Dresden, Institut für Planetare Geodäsie, Dresden, Germany
[2]Alfred Wegener Institute, Helmholtz Centre for Polar and Marine Research, Bremerhaven, Germany
[3]Institute for Marine and Atmospheric Research Utrecht, Utrecht University, Utrecht, The Netherlands

Correspondence to: Ludwig Schröder (ludwig.schroeder@tu-dresden.de)

Abstract. We developed a multi-mission satellite altimetry analysis over the Antarctic Ice Sheet which comprises Seasat, Geosat, ERS-1, ERS-2, Envisat, ICESat and CryoSat-2. After a consistent reprocessing and a stepwise calibration of the inter-mission offsets, we obtain monthly grids of multi-mission surface elevation change (SEC) w.r.t with respect to the reference epoch 09/2010. A validation with independent SEC from in situ elevation changes from in situ and airborne observations as well as a comparison with a firn model proves that the different missions and observation modes have been successfully combined to a seamless multi-mission time series. For coastal East Antarctica, even Seasat and Geosat provide reliable information and, hence, allow to analyze four decades of elevation changes. The spatial and temporal resolution of our result allows to identify when and where significant changes in elevation occurred. These time series add detailed information to the evolution of surface elevation in key regions as Pine Island Glacier, Totten Glacier, Dronning Maud Land or Lake Vostok. After applying a density mask, we calculated time series of mass changes and find that the Antarctic Ice Sheet north of 81.5°S lost a total mass of -2068was losing mass at an average rate of -85±37716 $\mathrm{Gt/yr}$ between 1992 and 2017. 2017, which accelerated to -137±25 $\mathrm{Gt/yr}$ after 2010.

1 Introduction

Satellite altimetry is fundamental for detecting and understanding changes in the Antarctic ice sheet (AIS, Rémy and Parouty, 2009; Shepherd et al., 2018). Since 1992, altimeter missions have revealed dynamic thinning of several outlet glaciers in West Antarctica and have put narrow limits on elevation changes in most parts of East Antarctica. Rates of surface elevation change are not constant in time (Shepherd et al., 2012). Ice flow acceleration has caused dynamic thinning to accelerate (Mouginot et al., 2014; Hogg et al., 2017). Variations in surface mass balance (SMB) and firn compaction rate also cause interannual variations of surface elevation (Horwath et al., 2012; Shepherd et al., 2012; Lenaerts et al., 2013). Consequently, different rates of change have been reported from altimeter missions that cover different time intervals. For example, ERS-1 and ERS-2 data over the interval 1992-2003 revealed negative elevation rates in eastern Dronning Maud Land and Enderby Land (25-60°E) and positive rates in Princess Elizabeth Land (70-100°E) (Wingham et al., 2006b), while Envisat data over the interval 2003-2010 revealed the opposite pattern (Flament and Rémy, 2012). Two large snowfall events in 2009 and 2011 have induced stepwise elevation changes in Dronning Maud Land (Lenaerts et al., 2013; Shepherd et al., 2012).

In consequence, results derived from a single mission, or even more so, mean linear rates reported from a single mission, have limited significance in characterizing the long-term evolution of the ice sheet (Wouters et al., 2013). Data from different altimeter missions need to be linked over a time span as long as possible in order to better distinguish and understand the long-term evolution and the natural variability of ice sheet volume and mass.

Missions with similar sensor characteristics were combined e.g. by Wingham et al. (2006b, ERS-1 and ERS-2) and Li and Davis (2008, ERS-2 and Envisat). Fricker and Padman (2012) use Seasat, ERS-1, ERS-2 and Envisat to determine elevation changes of Antarctic ice shelves. They apply constant biases, determined over open ocean, to cross-calibrate the missions. In contrast to ocean-based calibration, Zwally et al. (2005) found significant differences for the biases over ice sheets with a distinct spatial pattern (see also Frappart et al., 2016). Also Khvorostovsky (2012) showed that the correction of inter-mission offsets over an ice sheet is not trivial. Therefore, Paolo et al. (2016) cross-calibrated ERS-1, ERS-2 and Envisat on each grid cell, using overlapping epochs, which is very similar to our approach for these missions. Linking different missions becomes even more challenging when different sensor characteristics are concerned, such as ICESat laser altimetry or CryoSat-2 interferometric Synthetic Aperture Radar (SARIn) mode, or when the missions do not overlap in time.

Here we present an approach to combine seven different satellite altimetry missions over the AIS. By a refined waveform retracking and slope correction of the radar altimetry (RA) data we ensure consistency of the surface elevation measurements and improve their precision by up to 50%. In the following stepwise procedure, we first process the measurements from all missions jointly using the repeat altimetry method. We then form monthly time series for each individual mission data set. Finally, we merge all time series from both radar and laser altimetry. For this last step, we employ different approaches of inter-mission offset estimation, depending on the temporal overlap or non-overlap of the missions and on the similarity or dissimilarity of their altimeter sensors.

We arrive at consistent and seamless time series of gridded surface elevation differences with respect to a reference epoch (09/2010). They represent three-month temporal averages sampled every month and an effective spatial resolution of about The resulting monthly grids with a 10 km spatial resolution were obtained by smoothing with a moving window over three months and a spatial gaussian weighting with $2\sigma = 20\,\mathrm{km}$sampled to a 10 grid. We evaluate our results and their estimated uncertainties by a comparison with independent in situ data sets, results from satellite gravimetry . We evaluate our results and results from regional atmospheric climate modelingtheir estimated uncertainties by a comparison with independent in-situ and airborne datasets, satellite gravimetry estimates, and regional climate model outputs. We illustrate that these time series of surface elevation change (SEC) allow to study geometry changes and derived mass changes of the AIS in unprecedented detail. For some examples as Pine Island Glacier , Totten Glacier, Shirase Glacier (Dronning Maud Land) and Lake Vostok, we demonstrate the benefits of the long time series The recent elevation changes of Pine Island Glacier in West Antarctica, Totten Glacier in East Antarctica, and Shirase Glacier of Dronning Maud Land in East Antarctica are put in context with the extended time series from satellite altimetry. Finally, we calculate ice sheet mass balances from these data for the respectively covered regions. A comparison with independent data indicates a high consistency of the different data sets but reveals also remaining discrepancies.

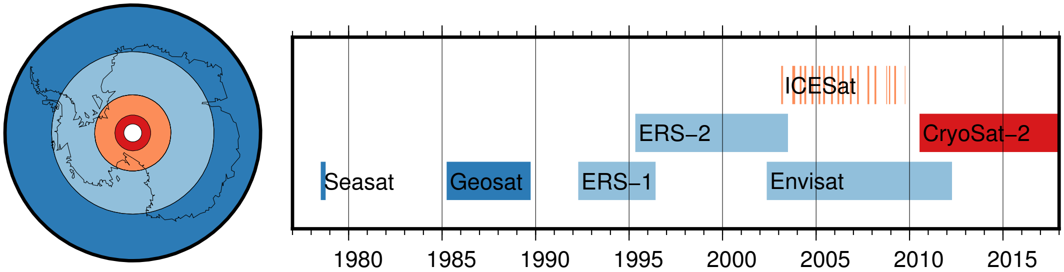

Figure 1. Spatial and temporal coverage of the satellite altimetry data used in this study. The colors denote the maximum southern extent of the measurements (dark blue: 72°S, light blue: 81.5°S, orange: 86°S, red: 88°S) and thus the size of the respective polar gap.

While this paper gives some examples for new insights obtained from the presented multi-mission altimetry analysis, it can not fully exploit all potential applications. This will be the scope of future work with this data set.

2 Data

2.1 Altimetry dataused

We use the ice sheet surface elevation observations from seven satellite altimetry missions: Seasat, Geosat, ERS-1, ERS-2, Envisat, ICESat and CryoSat-2. Figure 1 gives an overview over their temporal and spatial coverage. The data of the two early missions, Seasat and Geosat, were obtained from the Radar Ice Altimetry project at Goddard Space Flight Center (GSFC). For ERS-1, the ESA missions, we used the data of the REAPER reprocessing project (Brockley et al., 2017) of ERS-1 and ERS-2, Envisat and the RA-2 Sensor and Geophysical Data Record (SGDR) of Envisat in version 2.1 and Baseline C Level 2I data of CryoSat-2the most recent ESA products were used. For ICESat the final release from . For ICESat we used GLA12 of release 633 from the National Snow and Ice Data Center (NSIDC). Further details concerning the National Snow and Ice Data Center (NSIDC) was used. Further details concerning the dataset versions used are given in the supplement. The data editing criteria, applied to remove corrupted measurements in a preprocessing step are explained there as welldata set versions used and the data editing criteria, applied to remove corrupted measurements in a preprocessing step are given in the supplement.

As illustrated in Fig. 1, due to the inclination of 108°, Seasat and Geosat measurements cover only the coastal regions of the East Antarctic Ice Sheet (EAIS) and the northern tip of the Antarctic Peninsula Ice Sheet (APIS) north of 72°S, which is about 25% of the total ice sheet area. With the launch of ERS-1, the polar gap was reduced to areas south of 81.5°S, resulting in a coverage of 79% of the area. The polar gap is even smaller for ICESat (86°S) and CryoSat-2 (88°S), leading to a nearly complete coverage of the AIS in recent epochs.

ERS-1 and ERS-2 measurements were performed in two different modes, distinguished by the width of the tracking time window and the corresponding temporal resolution of the recorded waveform. The ice mode is coarser than the ocean mode, in order to increase the chance of capturing the radar return from rough topographic surfaces (Scott et al., 1994). While the ice mode was employed for the majority of measurements, a significant number of observations has been performed in ocean mode over Antarctica as well (22% for ERS-1, 2% for ERS-2). We use the data from both modes, as the ocean mode provides a higher precision while the ice mode is more reliable in steep terrain (see Fig. S1 and S3). However, as there is a regionally varying bias between the modes, we treat them as two separate data sets, similar to Paolo et al. (2016).

2.2 Reprocessing of radar altimetry

Compared to measurements over the global oceans, pulse limited radar altimetry (PLRA) over ice sheets requires a specific processing to account for the effects of topography and the dielectric properties of the surface (Bamber, 1994). To ensure consistency in the analysis of PLRA measurements, processed and provided by different institutions, we applied our own method for retracking and slope correction.

The slope correction is applied to account for the effect of topography within the beam limited footprint (Brenner et al., 1983). Different approaches exist to apply a correction (Bamber, 1994) but it is still a main source of error in RA . In Schröder et al. (2017) we showed the clear superiority of the this effect is still a main source of error in RA over ice sheets. The "direct method" uses the surface slope within the beam limited footprint to obtain a correction for the measurement in nadir direction. In contrast, the "relocation method" , which tries to relate the measurements to the true measurement position , over the "direct method ", which determines a correction for the nadir direction. Roemer et al. (2007) developed a refined relocation relates the measurement towards the likely true position up slope. While the direct method which locates the has the advantage that the measurement location is unchanged, which allows an easier calculation of profile crossovers or repeat track parameters, the relocation method has lower intrinsic errors (Bamber, 1994). A validation using crossovers with kinematic GNSS-profiles (Schröder et al., 2017) showed that, especially in coastal regions, the direct method leads to a significantly lager offsets and standard deviations, compared to the relocation method. Roemer et al. (2007) developed a refined version of the relocation method, using the full information of a digital elevation model (DEM) to locate the Point of Closest Approach (POCA) within the approximately 20 km beam limited footprintin a digital elevation model (DEM). We applied this method in our reprocessing chain using the DEM of Helm et al. (2014). The CryoSat-2 measurements, used for this DEM, have a very dense coverage, and hence, very little interpolation is necessary. Compared to the DEM of Bamber et al. (2009), this significantly improves the spatial consistency. We optimized the approach of Roemer et al. (2007) with respect to computational efficiency for the application over the entire ice sheet. Instead of searching the POCA with the help of a moving window of 2 km (which represents the pulse limited footprint) in the DEM-to-satellite grid, we applied a Gaussian filter with σ=1 km to the DEM itself to resemble the coverage of a pulse limited footprint. Hence, instead of the closest window average, we can simply search for the closest cell in the smoothed grid, which we use as coarse POCA location. In order to achieve a sub-grid POCA location, we fit a biquadratic function to the satellite-to-surface distance within a 3x3 grid cell environment around the coarse POCA grid cell and determine the POCA according to this function.

The retracking of the return signal waveform is another important component in the processing of RA data over ice sheets (Bamber, 1994). Functional fit approaches (e.g. Martin et al., 1983; Davis, 1992; Legrésy et al., 2005; Wingham et al., 2006b) are well established and allow the interpretation of the obtained waveform shape parameters with respect to surface and subsurface characteristics (e.g. Lacroix et al., 2008; Nilsson et al., 2015). However, the alternative approach of threshold retrackers has proven to be more precise in terms of repeatability (Davis, 1997; Nilsson et al., 2016; Schröder et al., 2017). A very robust variant is called ICE-1, using the "Offset Center of Gravity" (OCOG) amplitude (Wingham et al., 1986). Compared to the waveform maximum, the OCOG-amplitude is significantly less affected by noise (Bamber, 1994). Davis (1997) compared different retrackers and showed that a threshold based retracker, especially with a low threshold as 10%, produces a remarkably higher precision, compared to functional fit based results. We implemented three threshold levels (10%, 20% and 50%) for the OCOG-amplitude which allowed us to analyze the influence of the choice of this level, similar to Davis (1997).

In addition to PLRA, we also use the SARIn mode data of CryoSat-2, reprocessed by Helm et al. (2014). The difference with respect to the processing by ESA mainly consisted in a refined determination of the interferometric phase and in the application of a threshold retracker(TFMRA).

2.3 Accuracy and precision

The accuracy of RA-derived ice surface elevation measurements has been assessed previously by a crossover comparison with independent validation data such as the ICESat laser observations (Brenner et al., 2007), airborne lidar (Nilsson et al., 2016) or ground based GNSS profiles (Schröder et al., 2017). These Besides the offset due to snow pack penetration and instrumental calibration over flat terrain, these assessments revealed that with increasingly rough surface topography, the RA measurements show systematically higher elevations than the validation data. This These topography related offsets can be explained by the fact that for surfaces that undulate within the ~20 km beam-limited footprint, the radar measurements tend to refer to local topographic maxima (the POCA), while the validation data from ground-based GNSS profiles or ICESat-based profiles represent the full topography. Besides these systematic offsets, also the standard deviation of differences between RA data and validation data is influenced by the surface roughness due to the significantly different sampling of the topography. While over flat terrains, most altimeter satellites perform better than The standard deviation of differences between RA data and validation data contains information about the measurement noise but is additionally influenced by the significantly different sampling of a rough surface as well. While over flat terrains, this standard deviation is below 50 cm , in coastal regions the standard deviations can reach ten meters and more for most satellite altimeter data sets, it can reach ten meters and more in coastal regions. However, both types of error relate to the different sampling of topography of the respective observation techniques. An elevation change, detected from within the same technique, is not influenced by these effects. Hence, with respect to elevation changes, not the accuracy but the precision (i.e. the repeatability) has to be considered.

This precision can be studied using intra-mission crossovers between ascending and descending profiles. Here, the precision of a single measurement is obtained by $\sigma_H = |\Delta H|/\sqrt{2}$ as two profiles contribute to this difference. To reduce the influence of significant real surface elevation changes between the two passes, we consider only crossovers with a time difference of less than 31 days. In stronger inclined topography, the precision of the slope correction dominates the measurement error (Bamber, 1994). Hence, to provide meaningful results, the surface slope needs to be taken into consideration. We calculate the slope from the CryoSat-2 DEM (Helm et al., 2014). The absence of slope-related effects on flat terrain allows to study the influence of the retracker (denoted as noise here). With increasing slope, the additional error due to topographic effects can be identified.

A comparison of the crossover errors of our reprocessed data and of the respective standard products (see supplement for details) standard products shows significant improvements achieved by our reprocessing. Figure 2 shows this comparison for Envisat

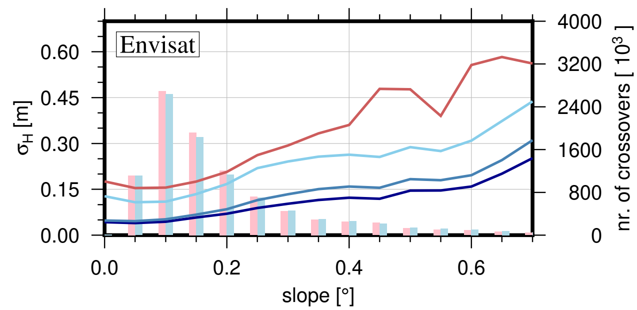

Figure 2. Precision of different processing versions of Envisat measurements from near time (<31 days) crossovers, binned against slope. Red curve: ESA version with ICE-2 retracker and relocated by mean surface slope. Light, medium and dark blue curves: Data reprocessed in this study with 50%-, 20%- and 10%-threshold retracker, respectively, relocated using the refined method. Vertical bars: number of crossovers for the ESA (red) and our 10% threshold retracked data (blue).

Table 1. Noise level and slope related component (s in degrees) of the measurement precision, fitted to near time crossovers (unit: m) of the data from the respective data center and our reprocessed data (with a 10% threshold retracker applied).

Data set	Data center	Reprocessed
Seasat	$0.21 + 1.91s^2$	$0.25 + 0.70s^2$
Geosat	$0.17 + 0.86s^2$	$0.18 + 1.16s^2$
ERS-1 (ocean)	$0.25 + 0.90s^2$	$0.09 + 0.18s^2$
ERS-1 (ice)	$0.36 + 2.37s^2$	$0.17 + 0.57s^2$
ERS-2 (ocean)	$0.23 + 0.75s^2$	$0.07 + 0.14s^2$
ERS-2 (ice)	$0.38 + 2.57s^2$	$0.15 + 0.53s^2$
Envisat	$0.17 + 1.03s^2$	$0.05 + 0.37s^2$
ICESat	$0.05 + 0.25s^2$	
CryoSat-2 (LRM)	$0.18 + 2.46s^2$	$0.03 + 1.06s^2$
CryoSat-2 (SARIn)	$0.38 + 2.01s^2$	$0.11 + 0.79s^2$

Note that the slope dependent component is weakly determined for data sets with a poor tracking in rugged terrain such as Seasat, Geosat or the ERS ocean mode and for the LRM mode of CryoSat-2.

(similar plots for each data set can be found in the supplement Fig. S1), binned into groups of 0.05° of specific surface slope. The results for a flat topography show that a 10% threshold provides the highest precision, confirming the findings of Davis (1997). For higher slopes, we see that also our refined slope correction contributed to a major improvement. A constant noise level σ_{noise} and a quadratic, slope related term σ_{slope} has been fitted to the respective data according to $\sigma_H = \sigma_{noise} + \sigma_{slope} \cdot s^2$, where s is in the unit of degrees. The results in Tab. 1 show that for each of the PLRA data sets of ERS-1, ERS-2 and Envisat, the measurement noise could be reduced by more than 50% compared to the ESA product (using the functional fit retracker ICE-2, see Legrésy and Rémy, 1997)which uses the functional fit retracker ICE-2 (Legrésy and Rémy, 1997). With respect to the CryoSat-2 CFI standard retracker (Wingham et al., 2006a), the improvement is even larger. Improvements are also significant for the slope-related component. For the example of Envisat and a slope of 1°, the slope-related component is 1.03 m for the ESA product and only 0.37 m for the reprocessed data. The advanced interferometric processing of the SARIn data achieved similar improvements. For the two early missions Seasat and Geosat, the crossover error of our reprocessed profiles is similar to that of the original dataset from GSFC. However, the number of crossover points is significantly increased, especially for Geosat (see Fig. S1). This means that our reprocessing obtained reliable data where the GSFC processor already rejected the measurements.

In addition to measurement noise, reflected in the crossover differences, a consistent pattern of offsets between ascending and descending tracks has been observed previously (A-D bias, Legrésy et al., 1999; Arthern et al., 2001). Legrésy et al. (1999) interpret this pattern as an effect of the interaction of the linearly polarized radar signal with wind-induced surface structures, while Arthern et al. (2001) attribute the differences to anisotropy within the snowpack. Helm et al. (2014) showed that a low threshold retracker significantly reduces the A-D bias. We observe a similar major reduction (from ±1 m in some regions for a functional fit retracker to ±15 cm when using a 10% threshold, see Fig. S2). The remaining bias is not larger, in its order of magnitude, than the respective noise. Moreover, near the ice sheet margins, the determination of meaningful A-D biases is complicated by the broad statistical distribution of A-D differences and the difficulty to discriminate outliers. We therefore do not apply a systematic A-D bias as a correction but rather include its effect in the uncertainty estimate of our final result.

3 Multi-mission SEC time series

Schematic diagram of the processing steps from the combined repeat track parameter fit over single-mission time series towards a combined multi-mission time series.

3.1 Repeat track parameter fit

We obtain elevation time series following the repeat track approach, similar to Legrésy et al. (2006) and Flament and Rémy (2012). As the orbits of the missions used here have different repeat track patterns, instead of along-track boxes we perform our fit on a regular grid with 1 km spacing (as in Helm et al., 2014). For each grid cell we analyze all elevation measurements h_i within a radius of 1 km around the grid cell center. This size seems reasonable as for a usual along track spacing of about 350 m for PLRA (Rémy and Parouty, 2009), each track will have up to 5 measurements within the radius. Due to the size of the pulse limited footprint a smaller search radius would contain only PLRA measurements with very redundant topographic information and thus would not be suitable to fit a reliable correction for the topography. As specified in Eq. (1), the parameters contain a linear trend (dh/dt), a planar topography (a_0, a_1, a_2) and a regression coefficient (dBS) for the anomaly of backscattered power ($bs_i - \overline{bs}$) to account for variations in the penetration depth of the radar signal.

For a single mission, the parameters are adjusted according to the model

$$\begin{aligned} h_i = \quad & dh/dt(t_i - t_0) + \\ & a_0 + a_1 x_i + a_2 y_i + \\ & dBS(bs_i - \overline{bs}) + \\ & res_i \end{aligned} \tag{1}$$

Here, t_i denotes the time of the observation. The reference epoch t_0 is set to 09/2010. x_i and y_i are the Polar Stereographic coordinates of the measurement location, reduced by the coordinates of the cell's center. The residual res_i describes the misfit between the observation and the estimated parameters.

To account for varying penetration depths due to variations in the electromagnetic properties of the ice sheet surface, different approaches exist. Wingham et al. (1998), Davis and Ferguson (2004), McMillan et al. (2014) or Zwally et al. (2015) apply a linear regression using the backscattered power. Flament and Rémy (2012), Michel et al. (2014) or Simonsen and Sørensen furthermore use two additional waveform shape parameters, obtained from functional fit retrackers. Nilsson et al. (2016) showed, that a low threshold retracker mitigates the need for a complex waveform shape correction. Hence, we decided to use a solely backscatter-related correction like the first group of authors did.

Besides the parameters in Eq. (1), McMillan et al. (2014) and Simonsen and Sørensen (2017) estimate an additional orbit direction related parameter to account for A-D biases. In Sect. 2.3 we showed that these biases are significantly reduced due to the reprocessing with a low threshold retracker. A further reduction of possible remaining artifacts of A-D biases is achieved by the smoothing in the merging step in Sect. 3.3.3. The weighted averaging of the results over a diameter of 60 km leads to a balanced ratio of ascending and descending tracks. Our choices concerning the correction for local topography, time-variable penetration effects and A-D biases were guided by the principle to prefer the simpler choice in doubt, in order to keep the number of parameters small compared to the number of observations.

In contrast to this single mission approach, here we perform a combined processing of all data from different missions and even different altimeter techniques. Thus, some of the parameters may vary between the data sets. To allow for offsets between the missions, the elevation at the cell center a_0 is fitted for each mission individually. The same applies to dBS, which might relate to specific characteristics of a mission as well. For Seasat, covering less than 100 days, this parameter is not estimated, as we assume that during the mission life time no significant changes occurred. For ICESat, dBS is not estimated either, as signal penetration is negligible for the laser measurements.

Between different observation techniques (i.e. PLRA, SARIn and laser altimetry), also the effective surface slope may differ. Considering the specific footprint sizes and shapes, the topography is sampled in a completely different way as illustrated in Fig. 3. While PLRA refers to the closest location anywhere within the ~20 km beam-limited footprint (i.e. the POCA), CryoSat's SARIn measurement can be attributed within the narrow Doppler stripe in cross-track direction. For ICESat the ~70 m laser spot allows a much better sampling of local depressions. Hence, the slope parameters a_1 and a_2 are estimated for each of the techniques independently.

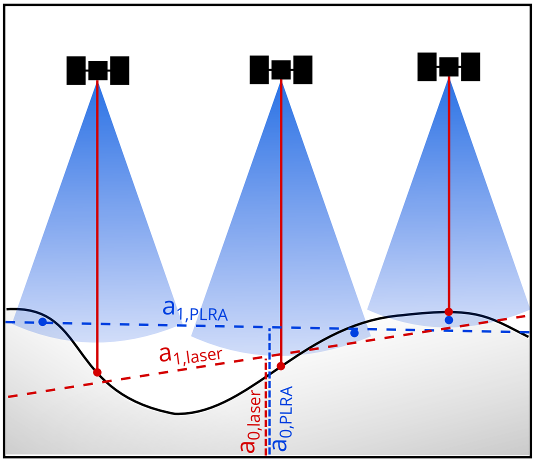

Figure 3. Illustration of the technique-dependent topographic sampling. The laser (red) measures the surface elevation in the nadir of the instrument while for radar altimetry (blue), the first return signal originates from the POCA (marked by the blue point). Hence, planar surface approximations to the measured heights (dashed lines) as in Eq. (2) are intrinsically different for the different techniques.

Considering these sensor-specific differences, the model for the least squares adjustment in Eq. (1) is extended for multi-mission processing

$$\begin{aligned} h_i = \quad & dh/dt(t_i - t_0) + \\ & a_{0,M(i)} + a_{1,T(i)}x_i + a_{2,T(i)}y_i + \\ & dBS_{M(i)}(bs_i - \overline{bs_{M(i)}}) + \\ & res_i \end{aligned} \tag{2}$$

where $M(i)$ and $T(i)$ denote to which mission or technique, respectively, the measurement h_i belongs.

We define a priori weights for the measurements h_i based on the precision of the respective mission and mode from crossover analysis (Tab. 1) and depending on the surface slope at the measurement location. This means that in regions with a more distinctive topography, ICESat measurements (with a comparatively low slope-dependent error component) will obtain stronger weights, compared to PLRA as Envisat. In contrast, over flat regions as on the East Antarctic plateau, the weights are very similar. Over regions of flat topography, such as the interior of East Antarctica, the weights between PLRA and ICESat are comparable

In order to remove outliers from the data and the results we apply different outlier filters. After the multi-mission fit, we screen the standardized residuals (Baarda, 1968), excluding any res_i which exceed five times its a posteriori uncertainty. We iteratively repeat the parameter fit until no more outliers are found. Furthermore, in order to exclude remaining unrealistic results from further processing, we filter our repeat track cells and reject any results where we obtain an absolute elevation change rate $|dh/dt|$ which is larger than 20 $\mathrm{m/yr}$ or where the standard deviation of this rate is higher than 0.5 $\mathrm{m/yr}$.

3.2 Single-mission time series

After fitting all parameters according to the multi-mission model (Eq. 2), we regain elevation time series by recombining the parameters a_0 and dh/dh with monthly averages of the residuals ($\overline{res}$). For each month j and each mission M, the time series is constructed as

$$h_{j,M} = a_{0,M} + dh/dt(t_j - t_0) + \overline{res_{j,M}}. \tag{3}$$

The elevations This recombination of parameters from Eq. (2) and averages of residuals does not include the parameters of topography slope and backscatter regression. Hence, each time series of $h_{j,M}$ all relate to the cells center and are relates to the cell center and is corrected for time-variable penetration , as the parameters of the topography slope and backscatter correction are omitted in this recombinationeffects. Due to the reference elevation $a_{0,M}$, which also contains may also contain the inter-mission offsets, offset, the penetration depth and a component of the topography sampling within the cell, this results in individual time series for each single mission. A schematic illustration of the results of this step is given in Fig. 5a. The temporal resolution of these time series is defined by using monthly averages . These of the residuals. With typical repeat cycle periods of 35 days or more, these $\overline{res}$ represent the anomalies of typically a single satellite pass towards all respective parameters including the linear rate of elevation change. The standard deviation of the residuals in these monthly averages are used as uncertainty measure for $h_{j,M}$ (see C.2 for further details).

3.3 Combination of the single-mission time series

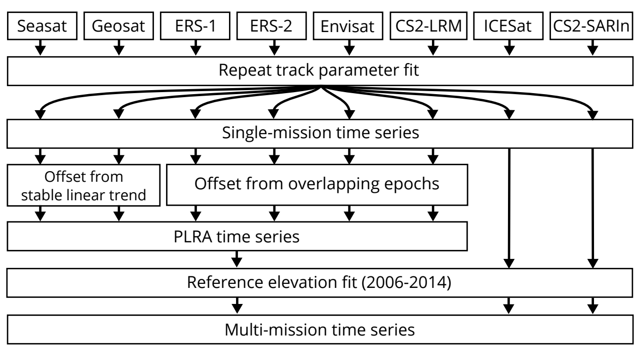

Figure 4. Schematic diagram of the processing steps from the combined repeat track parameter fit over single-mission time series towards a combined multi-mission time series.

In order to merge data from different missions into a joint time series, inter-mission offsets have to be determined and eliminated. In the ERS reprocessing project (Brockley et al., 2017), mean offsets between the ERS missions and Envisat have been determined and applied to the elevation data. However, for ice sheet studies inter-satellite offsets are found to be regionally varying (Zwally et al., 2005; Thomas et al., 2008; Khvorostovsky, 2012). When merging data from different observation techniques (PLRA, SARIn and laser) the calibration gets even more challenging. We chose an approach in different steps

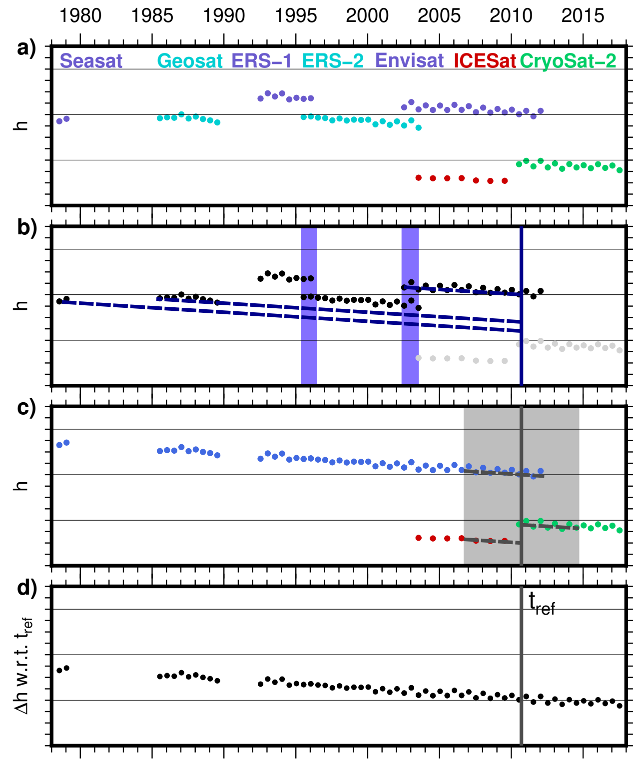

Figure 5. Schematic illustration of the combination of the missions. **a)** Single-mission time series of PLRA missions (blue and cyan), CryoSar-2 in SARIn mode (green) and the laser altimetry measurements of ICESat (red) with inter-mission offsets. **b)** Offsets between the PLRA data are determined from overlapping epochs (blue area) or trend-corrected elevation differences (according to Eq. 2) where dh/dt is sufficiently stable. **c)** The specific offset between PLRA, SARIn and laser data depends on the sampling of the topography within each single cell. These different techniques are aligned by reducing each elevation time series by the specific elevation at the reference epoch t_{ref}. Due to possible non-linear surface elevation changes, this reference elevation is obtained from a 8-year interval only (gray area). **d)** The combined multi-mission time series contains SECs with respect to t_{ref}.

which is depicted in Figs. 4 and 5. Further details concerning the processing of The following section gives an overview and explains the different steps to merge the single mission time series. A detailed description of the parameters used in each step can be found in the supplement.

3.3.1 Merging PLRA time series

In a first step, we merge the PLRA time series. For these missions the topographic sampling by the instruments is similar and thus the offsets are valid over larger regions. For overlapping missions (ERS-1, ERS-2, Envisat, CryoSat-2 LRM) the offsets are calculated from simultaneous epochs (blue area in Fig. 5b), as performed by Wingham et al. (1998) or Paolo et al. (2016). Smoothed grids of these offsets are generated, summed up if necessary to make all data sets comparable with Envisat (see Fig. S4) and applied to the respective missions. For the ERS missions, we find significant differences in the offsets for ice and ocean mode, hence, we determine separate offsets for each mode. Comparing our maps with similar maps of offsets between ERS-2 (ice mode) and Envisat shown by Frappart et al. (2016) reveals that the spatial pattern agrees very well but we find significantly smaller amplitudes. We interpret this as a reduced influence of volume scattering due to our low retracking threshold. In accordance with Zwally et al. (2005), we did not find an appropriate functional relationship between the offset and the waveform parameters.

To calibrate Geosat and Seasat, a gap of several years without observations has to be bridged. As depicted by the dashed blue lines in Fig. 5b, we do this using the trend corrected reference elevations $a_{0,M}$ from the joint fit in Eq. (2). This, however, can only be done if the rate is sufficiently stable over the whole period. Therefore, we use two criteria. First, we check the standard deviation of the fit of dh/dt. This $\sigma_{dh/dt}$ indicates the consistency of the observations towards a linear rate during the observational period. However, anomalies during the temporal gaps between the missions (i.e. 1978-1985 and 1989-1992) cannot be detected in this way. Therefore, we furthermore utilize a firn densification model (FDM, Ligtenberg et al., 2011; van Wessem et al., 2018). This model describes the anomalies in elevation due to atmospheric processes against the long-term mean. The RMS of the FDM time series is hence a good measure for the magnitude of the non-linear variations in surface elevation. Consequently, only cells where $\sigma_{dh/dt} < 1\,\mathrm{cm/yr}$ and $RMS_{FDM} < 20\,\mathrm{cm}$, indicating a highly linear rate, are used to calibrate the two historic missions. Maps of the offsets with respect to Envisat are shown in the supplement Fig. S5. Regions where this stability criterion is fulfilled are mainly found on the plateau. The mean values The FDM criterion is not able to detect changes in ice dynamics. However, as regions where both stability criteria are fulfilled are mainly found on the plateau where flow velocity are below 30 $\mathrm{m/yr}$ (Rignot et al., 2017), we expect no significant non-linear elevation changes due to ice flow. The mean of the offsets over all cells amounts to -0.86 m for Seasat and -0.73 m for Geosat. The corresponding standard deviations of 0.85 m and 0.61 m respectively are mainly a result of the regional pattern of the offsets. The true offsets are likely to have spatial variations. However, we are not able to distinguish spatial variations of the offset from residual effects of temporal height variations in the regions meeting the stability criterion. In the regions not meeting this criterion, we are not able to estimate the spatial variations of the offset at all. Therefore, our final estimate of the offset, applied to the measurements, is a constant, calculated as the average offset over the regions meeting the stability criterion. The spatial variability not accounted for by the applied offset is included, instead, in the assessed uncertainty. Our bias between Seasat and Envisat (-0.86±0.85 m) agrees within uncertainties with the ocean-based bias of -0.77 m used by Fricker and Padman (2012). However, we prefer this offset as the observed medium plays an important role for these biases (see Sect. C.3the offset determined over the ice sheet because this kind of offsets may depend on the reflecting medium (see Sect. C.2.2 for a more detailed discussion).

With the help of these offsets, all PLRA missions were corrected towards the chosen reference mission Envisat. Uncertainty estimates of the offsets are applied to the respective time series to account for the additional uncertainty. Hence, the PLRA time series are combined (blue in Fig. 5c with additional CryoSat-2 LRM mode where available). At epochs when more than one data set exists, we apply weighted averaging using the uncertainty estimates.

3.3.2 Technique-specific surface elevation changes

In contrast to the PLRA data in the previous step, when merging data from different observation techniques such as CryoSat's SARIn mode, ICESat's laser observations and PLRA, also the different sampling of topography has to be considered. As noted in Sect. 3.1 this might lead to completely different surfaces fitted to the respective each type of elevation measurements and thus, the time series need to be calibrated for each cell individually. However, not all cells have valid observations of each data set. Therefore, instead of calibrating the techniques against each other, we reduce each time series by their respective elevation at a common reference epoch and hence obtain time series of surface elevation changes (SEC) w.r.t. this reference epoch instead of absolute elevation time series. This step eliminates offsets due to differences in firn penetration or due to the system calibration between the techniques as well.

We chose September 2010 as the reference epoch. This epoch is covered by the observational periods of PLRA and CryoSat SARIn and also is exactly one year after the last observations of ICESat, which reduces the influence of an annual cycle. As discussed in Sect. 3.3.1, non-linear elevation changes will adulterate a_0 from Eq. (2), obtained over the full time span. Therefore, we applied another linear fit to a limited time interval of 8 years only (09/2006-09/2014, gray area in Fig. 5c). We subtract the variation of the FDM over this period to account for short-term variations. The limited time interval reduces the influence of changes in ice dynamics. We estimate the individual reference elevations $a_{0,T}$ for each technique T and a joint dh/dt. After subtracting the technique-specific reference elevations $a_{0,T}$ from the respective time series, they all refer to 09/2010 and can be combined.

3.3.3 Merging different techniques

We perform the final combination of the techniques using a weighted spatio-temporal averaging with $10\,\mathrm{km}$ σ gaussian weights in spatial domain (up to a radius of $3\sigma = 30\,\mathrm{km}$) and over 3 epochs (i.e. including the two consecutive epochs) in the temporal domain. Hence, we obtain grids of surface elevation change (SEC) with respect to 09/2010 for each month observed. Due to the smoothing of the weighting function, we reduce our spatial SEC grid resolution to $10\,\mathrm{x}\,10\,\mathrm{km}$. The respective uncertainties are calculated according to the error propagation. To avoid extrapolation and to limit this merging step to the observed area only, we calculate a value for the respective an epoch in the $10\,\mathrm{x}\,10\,\mathrm{km}$ grid cells only if we have data within $20\,\mathrm{km}$ around the cells center (which is about the size of a beam-limited radar footprint). The five examples in Fig. 6 demonstrate the spatio-temporal coverage of the resulting SEC grids at different epochs. The respective corresponding uncertainty estimates, given in Fig. 6b (further details in the supplement) reach values of one meter and more. Especially in the coastal regions, these uncertainty estimates of our SECs are not defined by the measurement noise and the uncertainty of the offset alone. In regions with fast elevation changes and a large spatial variation in the signal (such as the flow lines of fast-flowing outlet glaciers), the $\sigma_{\Delta h}$ also comprises the variation of the Δh within the area used for smoothingweighted averaging. This holds especially true for epochs that are far away from the reference epoch and, hence, have large values of Δh. Consequently, the epoch 09/2008 provides the lowest uncertainty estimate in these examples, even lower than the CryoSat-2 based epoch 09/2017.

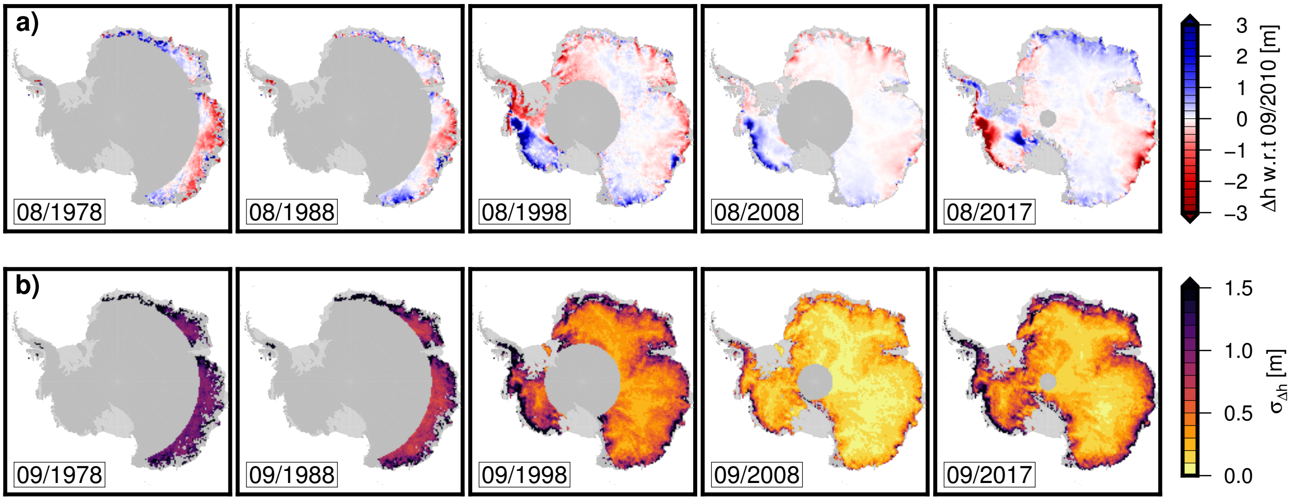

Figure 6. Five example snapshots of the resulting combined surface elevation time series (**a**) and their respective corresponding uncertainty (**b**). The height differences refer to our reference epoch 09/2010.

4 Comparison of SEC with independent data

4.1 In situ and airborne observations

To validate our results, we used inter-profile crossover differences of 19 kinematic GNSS profiles (Schröder et al., 2017) and elevation differences from Operation IceBridge (OIB ATM L4, Studinger, 2014). The ground based GNSS profiles have been observed between 2001 and 2015 on traverse vehicles of the Russian Antarctic Expedition and most of them cover more than 1000 km. The accuracy of these profiles has been determined in Schröder et al. (2017) to 4-9 cm. One profile (K08C) has not been used as the poorly determined antenna height offset might impose larger errors. For each crossover difference between kinematic profiles from different years, we compare the differences of the respective corresponding altimetric SEC epochs in this location ($\delta\Delta h = \Delta h_{KIN} - \Delta h_{ALT}$). The same analysis has been performed with the elevation changes from OIB. obtained from differences of measurements of the scanning laser altimeter (Airborne Topographic Mapper, ATM) of OIB. As described by Studinger (2014), the Level 4 Δh product is obtained by comparing planes fitted to the laser scanner point clouds. The flights, carried out between 2002 and 2016, were strongly concentrated along the outlet glaciers of West Antarctica and the Antarctic Peninsula. Hence, they cover much more rugged terrain which is more challenging for satellite altimetry. Nevertheless, over the tributaries of the Amundsen Sea glaciers and along the polar gap of ICESat, some repeated measurements have also been performed over flat terrain. Over summit station in Greenland, Brunt et al. (2017) validated such measurements with ground based GNSS profiles of snowmobiles and obtained offsets in the order of only a few centimeters and standard deviations between 4 and 9 cm.

Figures 7a and d show the results of this validation . our validation (more detailed maps for several regions at Fig. S6). A satellite calibration error would lead to systematic biases between the observed elevation differences if Δh_{ALT} is obtained

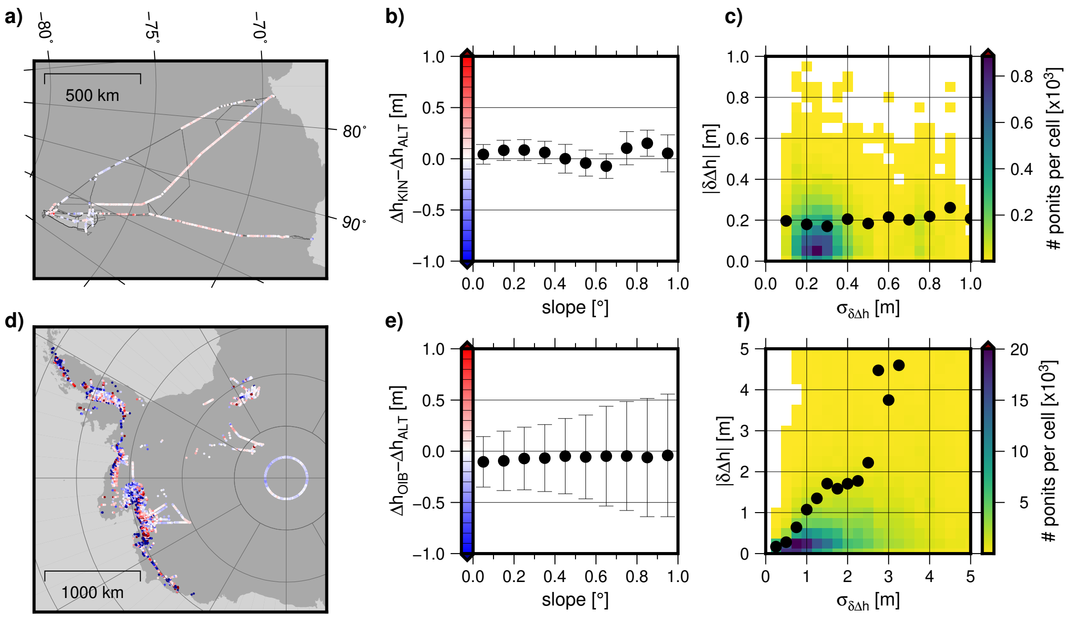

Figure 7. Validation with elevation differences observed by kinematic GNSS between 2001-2015 (**a,b,c**) and Operation IceBridge between 2002-2016 (**d,e,f**). Differences between elevation changes observed by the validation data and altimetry are shown on the maps (**a,d**, color scale in **b,e**). Median and MAD of these differences, binned by different surface slope, are shown in the center (**b,e**). The right diagrams (**c,f**) show the comparison of these differences with the respective uncertainty estimate, obtained from both data sets. The point density is plotted from yellow to blue and the black dots show the root mean square, binned against the estimated uncertainty.

from data of two different missions. However, such biases may also be caused by systematic errors in the validation data. Furthermore, in contrast to the calibration data, the RA measurements may systematically miss out regions which are changing most rapidly if they are located in a local depression some of the most rapid changes if those are located in local depressions (Thomas et al., 2008). With an overall median difference of 6±10 cm for the GNSS profiles and -9±42 cm for OIB, however, the observed elevation changes show only moderate systematic effects and agree within their error bars. The median absolute deviation (MAD) for different specific surface slopes (Fig. 7b and e) reveal the influence of topography in this validation. The GNSS profiles show only a very small increase of this variation with slope. The IceBridge data covers the margins of many West Antarctic glaciers, where elevation changes differ over relatively short distances. Hence, it is not surprising that we see a significantly larger spread of $\delta\Delta h$ at higher slopes here. However, also for the flat interior, the MAD of the differences is still at a level of 25 cm, which is significantly larger than in the comparison with the GNSS profiles. Brunt et al. (2018) report that the observations of the 2016 campaign of ICEBridge show a systematic offset due to a bias in the instrumental orientation around the 88°S circle, which could explain the systematic differences there.

The observed $\delta\Delta h$ can further be used to evaluate the uncertainty estimate of the respective elevation differencesestimates. In Fig. 7c and f, the uncertainty estimates of the four contributing data are combined and compared to the observed differences. The comparison with both datasets shows that these estimates seem reasonable. In the comparison with the GNSS profiles, the relatively low differences, even in regions which imply a higher uncertainty, are likely just incidental for the small sample of $\delta\Delta h$ validation data sets supports that the uncertainty estimates are reasonable. For Δh_{ALT} we expect higher errors in coastal regions due to the increased uncertainty of the topographic correction in radar altimetry. A similar relation to topography is expected for Δh_{OIB} due to the plane fit to the ATM point cloud. In contrast, the errors of the GNSS-derived Δh_{KIN} are almost independent of topography. Instead, Δh_{KIN} tends to be more uncertain on the plateau, where the soft snow causes large variations of the subsidence of the vehicles into the upper firn layers. The relatively low differences in $\delta\Delta h$ even in regions that imply a higher uncertainty, are likely just incidental for the small sample of validation data along the GNSS profiles.

In conclusion, this validation shows that remaining systematic biases (originating from satellite altimetry or the validation data) are on a centimeter level only and that our uncertainty estimate is realistic. However, we have to stress that less than a decimeter in the observed regions and that our uncertainty estimate is realistic. However, only altimetric SEC within the interval 2001-2016 can be validated in this way. For the earlier missions, no spatially extensive high precision in situ data are available to uspublicly available.

4.2 Firn model

Another data setwhich covers almost the identical spatial and temporal range as the altimetric data is the firn thickness data set of the IMAU Firn Densification Model (FDM Ligtenberg et al., 2011), which covers almost the identical spatial and temporal range as the altimetric data, is the IMAU Firn Densification Model (FDM, Ligtenberg et al., 2011), forced at the upper boundary by accumulation and temperature of the Regional Atmospheric Climate Model, version 2.3p2 (van Wessem et al., 2018). Before we can compare this model to our SEC results, however, it is important to mention that the FDM only contains elevation anomalies . A The IMAU-FDM has been updated to the period 1979-2016, modeling the firn properties and the related surface elevation changes on a 27 km grid. However, as the FDM contains elevation anomalies only, any long-term elevation trend over 1979-2016, e.g. due to changes in precipitation on longer time scales (Thomas et al., 2015) (as e.g. observed in some regions of West Antarctica, Thomas et al., 2015) would not be included in the model. Furthermore, due to the nature of the model, it cannot give information about ice dynamic thinning/thickening. Hence, to compare the FDM and the SEC from altimetry, we first remove a linear trend from both data sets respectively. This is performed for the period 1992-2016 . (depicted in Fig. S7). The trends are only calculated from epochs where both data sets have data, i.e. in the polar gap this comparison is limited to 2003-2016 or 2010-2016, depending on the first altimetry mission providing data here. After the detrending, the anomalies are used to calculate correlation coefficients for each cell, depicted in Fig. 8a. Figure 8b shows the RMS of these anomalies from the altimetry data, representing the magnitude of the seasonal and interannual variations average magnitude of the seasonal and interannual variations (non-linear SEC), calculated as the RMS of the anomalies from the altimetry data. Comparing the two maps shows that the correlation is around 0.5 or higher, except in regions where the magnitude of the anomalies is small, i.e. where the signal-to-noise ratio of the altimetric data is low. This relationship is depicted in Fig. 8c, where we see that for the vast majority of cells the correlation is positive. For anomalies with a RMSnon-linear SEC > 0.5 m, the average correlation is between 0.3 and 0.6.

Anomalies against the simultaneously observed long-term trend (1992-2016) can also be computed for earlier epochs. Assuming no significant changes in ice dynamics here, these anomalies allow a comparison of Geosat and Seasat with the FDM. The median difference between the anomalies according to Geosat and the anomalies according to the FDM amounts to

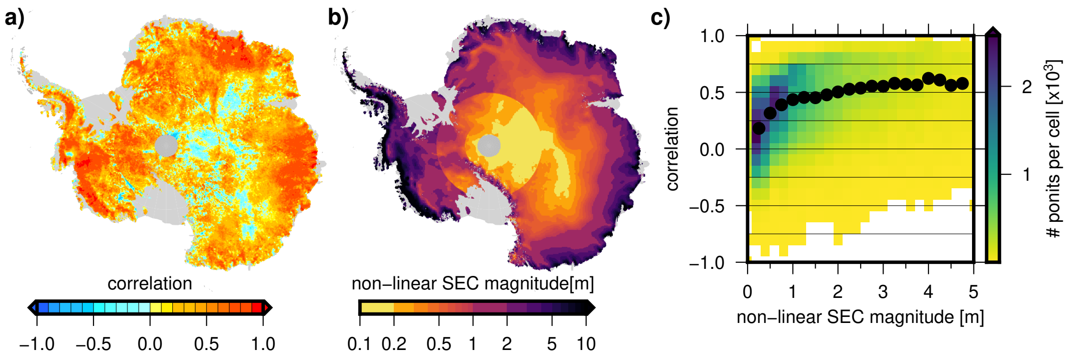

Figure 8. a) Correlation coefficient between the SEC anomalies of the altimetry grids and the FDM over 1992-2016 after detrending. **b)** RMS average magnitude of the detrended anomalies of the 1992-2016 altimetry time series. **c)** Correlation coefficient plotted against the RMSnon-linear SEC. The point density is color coded from yellow to blue. The black dots show the binned mean values.

0.12±0.21 m (see Fig. S6). Considering that this difference is very sensitive to extrapolating the respective S8). Considering that this difference is very sensitive to extrapolating the long-term trends, this is a remarkable agreement. With a median of 0.26±0.32 m, the difference between anomalies from Seasat and from the FDM is larger, but this comparison is also more vulnerable to potential errors due to the extrapolation. As the FDM starts in 1979 while Seasat operated in 1978, we compare the Seasat data with the FDM anomalies from the respective months of 1979, which might impose additional differences. Finally, the FDM model has its own inherent errors and uncertainties. Therefore, only part of the differences originates from errors in the altimetry results.

5 Results

5.1 Surface elevation changes

The average rates of elevation change over different time intervals of our multi-mission time series are shown in Fig. 9. To calculate these rates, we first averaged the data over the first year and the last year of the interval to reduce the noise, then subtracted the respective averages from each other and finally divided these differences by their time difference in years. If one of the years does not cover the full annual cycle, we calculate the average only from the months covered in both years (July-October for 1978-2017, April-December for 1992-2017). We calculate the SEC rate from epoch differences instead of fitting a rate to all epochs because the first observations at specific latitudes start in different years, the observations have different precisions and the large gap between 1978 and 1985 is not covered by observations at all. These three points would lead to a bias towards the later epochs in a fit, so that the rates would not be representative for the true average elevation change over the full interval.

The long-term elevation changes over 25 years (Fig. 9b) show the well known thinning in the Amundsen Sea Embayment and at Totten Glacier, as well as the thickening of Kamb Ice Stream (cf. e.g. Wingham et al., 2006b; Flament and Rémy, 2012; H . In contrast, 60% of East Antarctica north of 81.5°S shows surface elevation changes of less than ±1 cm/yr. Several

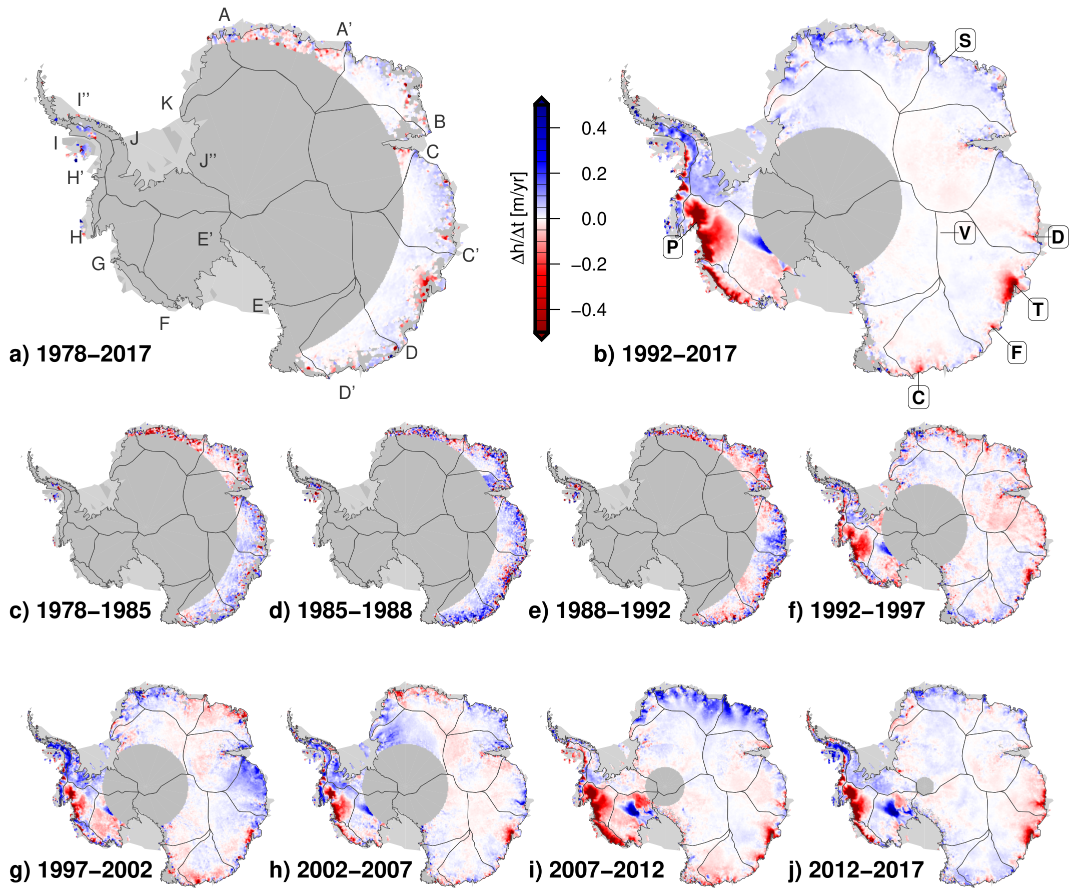

Figure 9. Multi-mission surface elevation change from the combined SEC time series over different time intervals. **a** and **b)** The long-term surface elevation change between 1978 and 2017 and 1992 and 2017 for the respectively covered area. **c-j)** Elevation change over consecutive time intervals reveal the interannual variability. Thin lines mark the drainage basin outlines, denoted in **a**. Bold letters in boxes in **b** denote areas mentioned in the text and in Fig. 10.

coastal regions of the EAIS, however, show significant elevation changes. Totten Glacier (T in Fig. 9b) is thinning at an average rate of 72±18 $\mathrm{cm/yr}$ at the grounding line (cf. Fig. 10b). Several smaller glaciers in Wilkes Land also show a persistent thinning. We observe SEC rates of -26±10 $\mathrm{cm/yr}$ at Denman Glacier (D), -41±19 $\mathrm{cm/yr}$ at Frost Glacier (F) and -33±12 $\mathrm{cm/yr}$ near Cook Ice Shelf (C). Rignot (2006) showed that the flow velocity of these glaciers, which are grounded well below sea level, was above the balance velocity for many years. Miles et al. (2018) analyzed satellite images since 1973 and found that the flow velocity of Cook Glacier has significantly accelerated since then. In contrast, the western sector of the EAIS (Coats Land, DML and Enderby Land; basins J”-B) shows thickening over the last 25 years at rates of up to a decimeter per year.

Comparing the long-term elevation changes over 40 years (Fig. 9a) with those over 25 years shows the limitations of the early observations, but also the additional information they provide. There were relatively few successful observations at the very margins. However, for Totten Glacier and Denman Glacier, the 40-year rates at a distance about 100 km from the grounding line are similar to the rates over the 1992-2017 interval. This indicates that the thinning there is very persistent. Figures 9c-j demonstrate another benefit of our merged time series. They allow to calculate rates over any sub-interval, independent of mission periods. The results over different intervals show that most of the coastal regions of the AIS experience significant interannual variations. Such large scale fluctuations in elevation change during the Envisat period have been reported by Horwath et al. (2012) or Mémin et al. (2015). Our combined multi-mission time series allow a detailed analysis of such signals on a temporal scale of up to 40 years.

Some examples for elevation change time series in the resulting multi-mission SEC grids are shown in Fig. 10 (coordinates in Tab. S2). For Pine Island Glacier (PIG, Fig. 10a), we observe a continuous thinning over the whole observational period since 1992 (Seasat and Geosat measurements do not cover this region). Close to the front did not cover this region). Close to the grounding line (point D) the surface elevation decreased by -45.8±7.8 m since 1992, which means an average SEC rate of -1.80±0.31 m/yr. The time series reveals that this thinning was not constant over time, but accelerated near the grounding line (point D and C at a distance of 40) around significantly around 2006. Also the points The mean rate at D over 1992-2006 of -1.32±0.66 m/yr increased to -4.17±1.67 m/yr over 2007-2010. After 2010, the thinning rates near the grounding line decelerate again and for the period 2013-2017, the rate at D of -1.31±0.80 m/yr is very close to the rate preceding the acceleration. Also at greater distances from the grounding line (B at 80 km, A at 130 km) show an acceleration we observe an acceleration of the prevailing rates around 2006. After 2010, the thinning rates at near front decelerate again. For the period 2013-2017, the rate of -1.3±0.82006 (-0.44±0.15 m/yr is very close to the rate preceding the acceleration. In contrast over 1992-2006, -1.20±0.10 m/yr over 2006-2017 at A). In contrast to the points near the grounding line, further inland the thinning did not decelerate so far and is still at a level of about -1.2 high level. Hence, for the most recent period (2013-2017) the elevation at all points along the 130 km of the main flow line is decreasing at very similar rates. A similar acceleration of the elevation change rate near the grounding line, followed by slowdown, is observed by (Konrad et al., 2016). The onset of this acceleration coincides with the detaching of the ice shelf from a pinning point (Rignot et al., 2014). After that speedup terminated around For the time after 2009, the grounding line position was relatively stable (Joughin et al., 2016), which agrees with the elevation changesin our observationsJoughin et al. (2016) report relatively little grounding line migration, resulting in a leveling off of the ice flow velocity. This agrees with our observed slowdown of elevation changes.

Also for Totten Glacier in East Antarctica (Fig. 10b), we observe a clear negative SEC. This has been previously reported by several authors (e.g. Pritchard et al., 2009; Flament and Rémy, 2012; Zwally et al., 2015) but our data provide an unprecedented time span and resolutiontemporal resolution, allowing to analyze the evolution of the elevation changes on a monthly scale over up to 40 years. At the very grounding line (point D), Totten Glacier thinned by 31.8±7.7 m between 1987 and 2017, which results in an average SEC rate of -1.0±0.2-1.03±0.25 m/yr. Seasat could not provide successful observations at the very grounding line but the time series for point C (around 60 km inland) with a rate of -0.38±0.10 m/yr between 1978 and 2017 and for point B (150 km) with a rate of -0.11±0.04 m/yr , respectively, indicate that this thinning already preceded before the epoch of Geosat. At point A in a distance of 280 km, we find no significant elevation change (0.01±0.03 m/yr for 1978-2017).

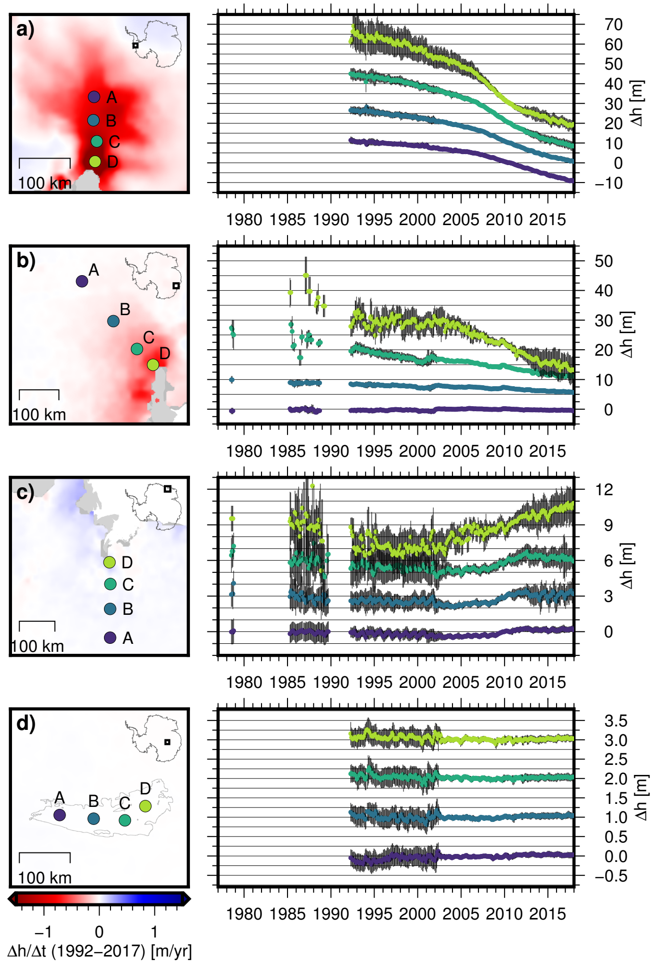

Figure 10. Multi-mission SEC time series in 4 selected regions (**a)** Pine Island Glacier, **b)** Totten Glacier, **c)** Shirase Glacier in Dronning Maud Land and **d)** Lake Vostok (marked by P, T, S and V in Fig. 9b). The time series of point B, C and D are shifted along Δh for better visibility and the one σ uncertainty range displayed in black. The maps on the left show the elevation change rate between 1992 and 2017 as in Fig. 9b (but in a different color scale).

The temporal resolution of these data allows us to analyze the change over time. While we see a significant thinning at the grounding line between 1987 and 1994 of 16.6±9.8 m, the elevation stabilized between 1994 and 2004 to within ±1.5 m. After 2004, the ice at the grounding line thinned again by 15.4±5.5 m until 2017. Li et al. (2016) observe a similar variation in ice velocity measurements between 1989 and 2015. Combining their ice discharge estimates with surface mass balance, they obtain a relatively large mass imbalance for Totten Glacier in 1989, decreasing in the following years to a state close to equilibrium around 2000. After 2000, they observe an acceleration of ice flow, again consistent with our thinning rates. The authors attribute this high variability to variations in ocean temperature. In another study, Li et al. (2015) observe a grounding line retreat at Totten Glacier of 1 to 3 km between 1996 and 2013 using SAR Interferometry. They conclude that this indicates a thinning by 12 m, which is again consistent with our results over this period (12.0±8.8 m).

At Shirase Glacier in Dronning Maud Land (DML, Fig. 10c), we observe a relatively stable surface with a slightly negative change rate between 1978 and the early 2000s. In this region, two significantly positive accumulation anomalies The sub-intervals until 2002 in the elevation change maps of Fig. 9c-g confirm that this agrees with the large scale trend in this region. After 2002, however, the elevation change switches the sign. Two significant accumulation events occurred in 2009 and 2011 (Boening et al., 2012; Lenaerts et al., 2013)in this region (Boening et al., 2012; Lenaerts et al., 2013). Our time series show an increasing surface elevation associated to these events. The increase in surface elevation associated to these event is visible in our time series. At point C, the elevation changed by 1.0±1.5 m between 2008 and 2012. Even at point A, more than 200 km inland and at an altitude of 2500 m, the elevation increased by 0.55±0.50 m during this time. At point D, a similar jump is an abrupt elevation increase is also observed in 2003, which corresponds to another SMB anomaly (cf. Fig. 2a in Lenaerts et al., 2013). The map in Fig. 9h shows that the coastal regions of Enderby Land (basin A'-B) already experienced elevation gains before 2007. In contrast to the 2009 and 2011 events, which affected a very large region (Fig. 9i), this earlier accumulation event is significantly more localized at the coast.

In contrast to the regions discussed so far, the elevation change on the plateau of East Antarctica is very small. The time series for four different points at Lake Vostok (Fig. 10d) show rates which are within uncertainties and very close to zero (point A: 5±9 mm/yr, B: -1±10 mm/yr, C: -3±9 mm/yr, D: -1±10 mm/yr between 1992 and 2017). The larger variations in the ERS time series is are a result of the lower resolution of the waveform in the ice mode of the ERS satellites. These rates contradict the findings of Zwally et al. (2015). They report a surface elevation increase of 20 mm/yr over Lake Vostok, which would result in an increase of elevation of elevation increase of 0.5 m over the period 1992-2017. Our results are confirmed by ground based static GNSS observations (Richter et al., 2008, 0.3±4.9 mm/yr), kinematic GNSS profiles measured around Vostok Station using snow mobiles (Richter et al., 2014, 1±5 mm/yr) and by GNSS profiles using traverse vehicles over the entire Lake Vostok region (Schröder et al., 2017, -1±5 mm/yr).

Multi-mission surface elevation change from the combined SEC time series over different time intervals. **a** and **b)** The long-term surface elevation change between 1978 and 2017 and 1992 and 2017 for the respectively covered area. **c-j)** Elevation change over consecutive time intervals reveal the interannual variability. Thin lines mark the drainage basin outlines, denoted in **a**. Bold letters in boxes in **b** denote glaciers, mentioned in the text.

The full pattern of surface elevation changes is shown in Fig. 9. These change rates are obtained by calculating elevation differences between the respective years, divided by the time difference. To reduce remaining noise, we use yearly averages (January-December). If one of the years does not cover the full annual cycle, we calculate the average only from the months covered in both years (July-October for 1978-2017, April-December for 1992-2017). We calculate the SEC rate from epoch differences instead of fitting a rate to all epochs because the first observations at specific latitudes start in different years, the observations have different precisions and the large gap between 1978 and 1985 is not covered by observations at all. These three points would lead to a bias towards the later epochs in a fit, which would not be representative for the true average elevation change over the full interval.

The long-term elevation changes over 25 years (Fig. 9b) show the well known thinning in the Amundsen Sea Embayment and at Totten Glacier, as well as the thickening of Kamb Ice Stream (cf. e.g. Wingham et al., 2006b; Flament and Rémy, 2012; Helm et al., 2014). In contrast, 60% of East Antarctica north of 81.5°S shows surface elevation changes of less than ±1 . However, several coastal regions of the EAIS show significant elevation changes, too. Totten Glacier (T in Fig. 9b) is thinning at an average rate of 72±18 at the

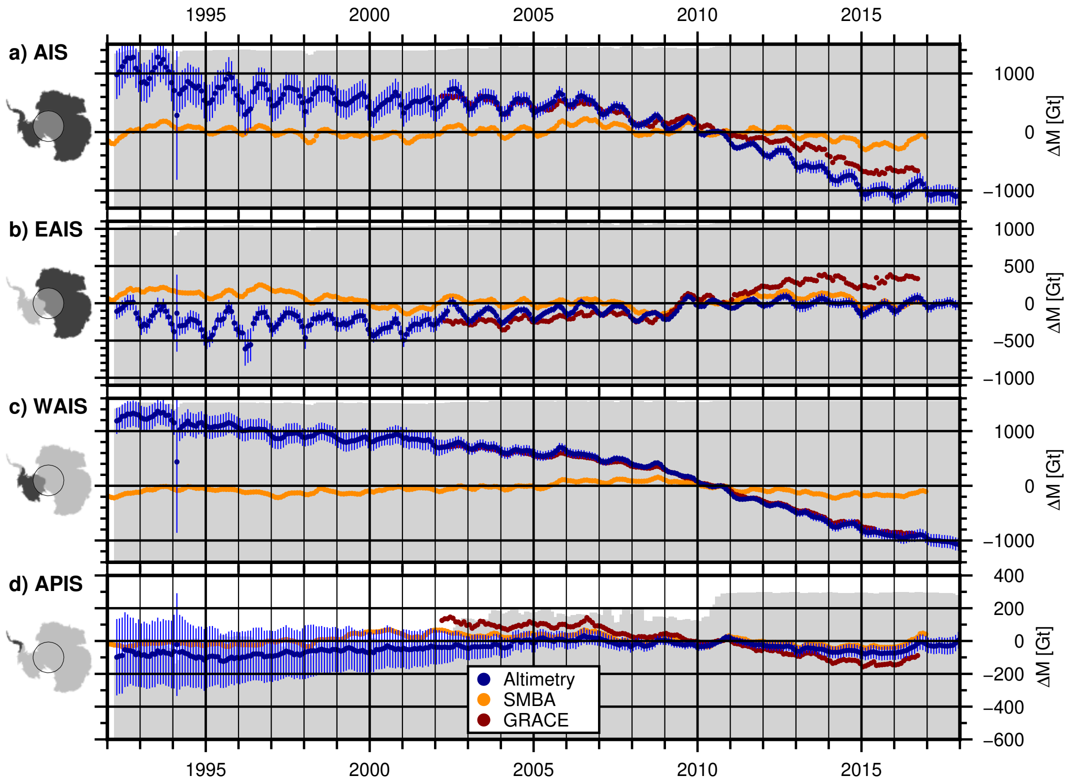

Figure 11. Mass change of the Antarctic Ice Sheet north of 81.5°S (**a**) and the three subregions (**b** EAIS, **c** WAIS and **d** APIS) from our combined altimetric time series (blue), GRACE (red) and SMB SMBA (orange). The error bars show the uncertainty estimate σ_Σ of the altimetry data according to Sect. F.2. The gray color in the background displays the fraction of the area covered by altimetry (up to the top means 100%).

grounding line (cf. Fig. 10b). Several smaller glaciers in Wilkes Land also a persistent thinning. We observe SEC rates of -26±10 at Denman Glacier (D), -41±19 at Frost Glacier (F) and -33±12 near Cook Ice Shelf. Rignot (2006) showed that the flow velocity of these glaciers, which are grounded well below sea level, was above the balance velocity for many years. In contrast, the western sector of the EAIS (Coats Land, DML and Enderby Land, basins J”-B) shows thickening over the last 25 years at rates of up to a decimeter per year.

Comparing the long-term elevation changes over 40 years (Fig. 9a) with those over 25 years shows the limitations of the early observations, but also the additional information they provide. There were only relatively few successful observations at the very margins but e.g. for Totten or Denman Glacier, they show similar rates at a distance of about 100 from the grounding line. In DML and Enderby Land (basins A-B in Fig. 9a), the 40 interval shows less positive rates, compared to 1992-2017. Until 2002, a large part of this region even experienced significant thinning (see time series in Fig. 10c and the maps for the sub-intervals in Fig. 9c-g). After that time, especially over the period 2007-2012 (Fig. 9i), this region shows a huge increase in elevation, which relates mainly to the accumulation events in 2009 and 2011. The sub-intervals in Fig. 9c-j demonstrate the effect of interannual snowfall variability on the elevation change rates over shorter time intervals. They show similar variations also in other regions, pointing out that accumulation events have a strong influence on interannual elevation changes over all parts of Antarctica (Horwath et al., 2012; Mémin et al., 2015).

5.2 Ice sheet mass time series

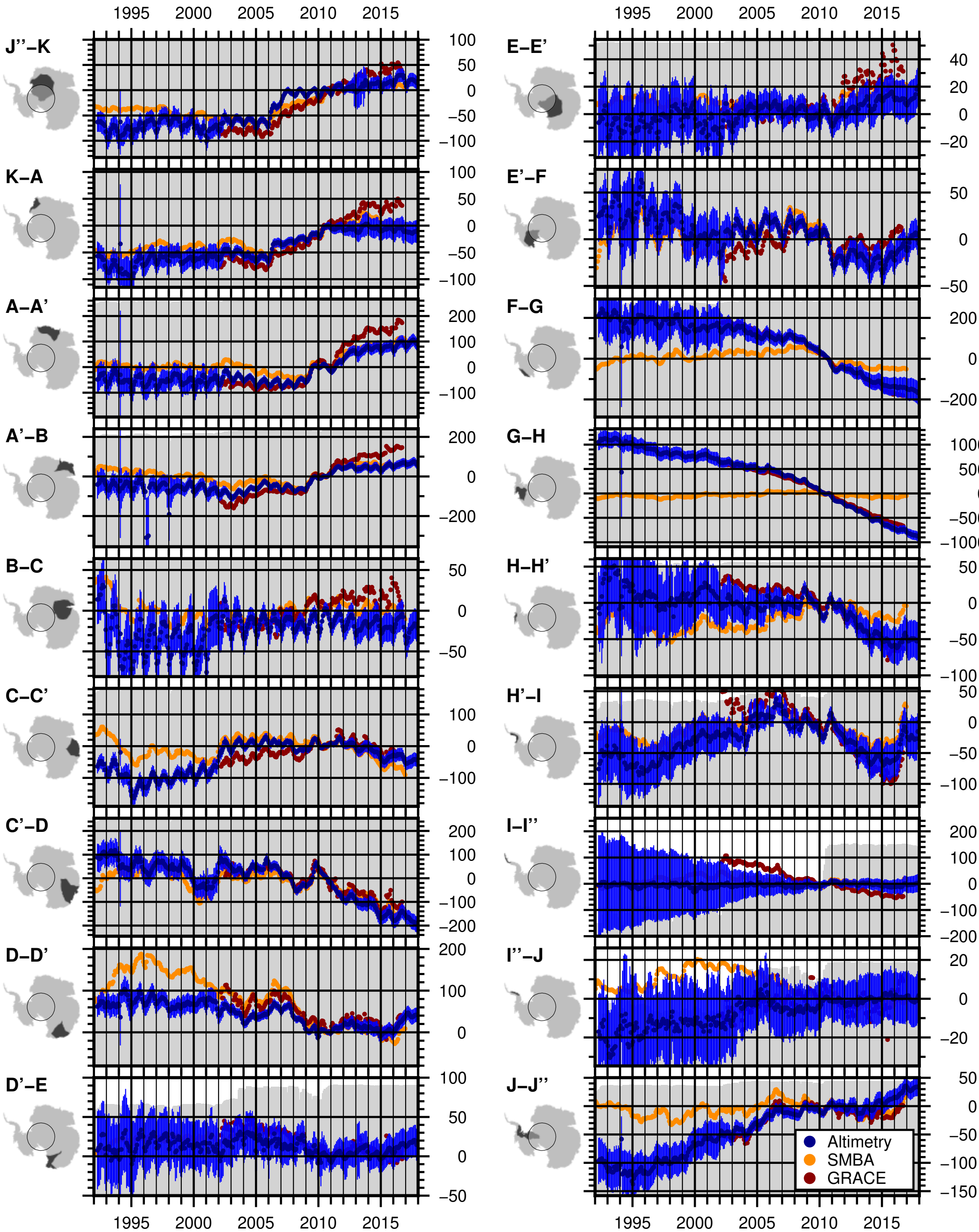

Figure 12. Mass change ($\Delta M[Gt]$) of the individual drainage basins north of 81.5°S from our combined altimetric time series (blue), GRACE (red) and SMB SMBA (orange). The error bars show the uncertainty estimate σ_Σ of the altimetry data according to Sect. F.2. The gray color in the background displays the fraction of the area covered by altimetry (up to the top means 100%).

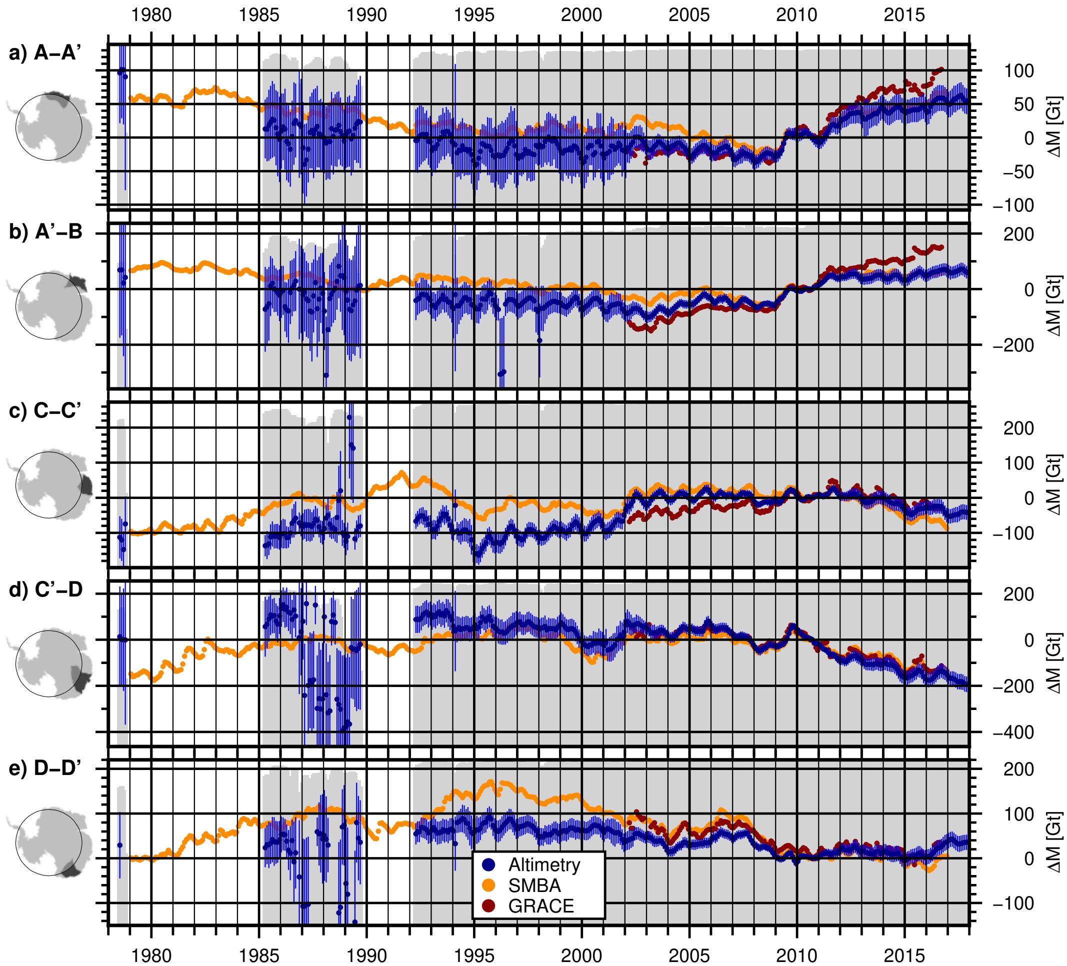

Figure 13. Mass change of subregions north of 72°S for several East Antarctic drainage basins from our combined altimetric time series (blue), GRACE (red) and SMB SMBA (orange). The error bars show the uncertainty estimate σ_Σ of the altimetry data according to Sect. F.2. The gray color in the background displays the fraction of the area covered by altimetry (up to the top means 100%).

In order to determine the effect of the SEC on global sea level, they are converted to ice mass changes. In a first step, all time series are corrected for glacial isostatic adjustment (GIA) using The surface elevation time series are converted into ice mass changes in order to determine their effect on global sea level. In a first step, the SECs are corrected for uplift rates related to glacial isostatic adjustment (GIA) using coefficients from the IJ05_R2 model (Ivins et al., 2013). This GIA model predicts an uplift of $5\,\mathrm{mm/yr}$ near the Antarctic Peninsula and rates between -0.5 and +2 $\mathrm{mm/yr}$ in East Antarctica. Furthermore we applied multiplied the SEC by a scaling factor $\alpha = 1.0205$ to account for elastic solid earth rebound effects (Groh et al., 2012). We multiply the resulting ice sheet thickness changes by each cell’s area and apply The resulting ice sheet thickness changes are multiplied by each cell’s area and a density according to a firn/ice mask (McMillan et al., 2014, 2016), depicted in Fig. S8S10, to obtain a mass change. In regions where ice dynamic processes are assumed to be dominating (e.g. in Amundsen Sea Embayment, Kamb Ice Stream or Totten Glacier), we use a density of 917 kg/m^3. Elsewhere, we apply the density of near-surface firn as modeled by Ligtenberg et al. (2011), using annual averages of accumulation, 10 m wind speed and surface temperature. We have chosen this straightforward method here, obtained from firn modeling using atmospheric forcing (Ligtenberg et al., 2011). We have chosen this straightforward and robust method here, instead of using modeled temporal variations instead of the firn layer (as e.g. Zwally et al., 2015; Kallenberg et al., 2017) in the volume-to mass conversion. This allows us to compare the time series from altimetry with time series from SMB modelingusing the modeled impact of the temporal variations of accumulation, melting and firn compaction on the firn layer (as e.g. Zwally et al., 2015; Kallenberg et al., 2017) in the volume-to-mass conversion. This allows us to keep our altimetry time series independent from the modeled variations in SMB, which is a prerequisite for the interpretation of the comparison of both data sets.

Cumulated mass anomalies over larger regions such as drainage basins or even the total AISare obtained by summing up the results accordingly. Therefore, we used the basin definitions by Rignot et al. (2011)(updated for Shepherd et al. (2018), see Figs. 9a and 14b). Cells containing no valid data after the gridding (as e.g. where not enough observations were available, in the polar gap or where rocks are predominant) are not considered here. Uncertainty estimates were obtained by propagating the respective We integrate our measurements over larger regions to calculate the cumulative mass anomalies for individual drainage basins and major Antarctic sectors (AIS, WAIS, EAIS, APIS). Our basin delineations are from Rignot et al. (2011), which have been updated for the second Ice Sheet Mass Balance Inter-comparison Exercise (IMBIE-2, Shepherd et al., 2018). Cells that were masked out due to the predominance of rocks or that are considered unobserved after our gridding (due to the polar gap or a lack of valid observations) are not included in these sums. Uncertainty estimates are obtained by propagating the uncertainties of the SEC, the GIA and the firn density to the basin sums for each month (see Sect. F.2 for details). We also include an estimate for the effect of unobserved cellsin To account for the lack of information due to unobserved cells, we also add a total estimate for the effect of these cells, based on trends from GRACE, to the error budget.

Figures 11a-d show time series for the entire AIS north of 81.5°S (i.e. covered by satellite altimetry since 1992), and the respective subregions EAIS, WAIS and the APIS. Similar time series for the single drainage basins over 1992-2017 are shown in Fig. 12. The full four decade time interval for the coastal areas of the EAIS For the coastal areas of the EAIS the full time interval since 1978 is shown in Fig. 13. These time series use the four decades time series use data north of 72°S only and, hence, provide a nearly consistent observational coverage since 1978. over the whole period. To support the interpretation and evaluate the temporal evolution, we compared the respective time series to GIA-corrected cumulated mass anomalies from satellite gravimetry (GRACE, Groh and Horwath, 2016) which are products of the ESA Climate Change Initiative (CCI) Antarctic Ice Sheet project and are available for download at https://data1.geo.tu-dresden.de/ais_gmb and http://cci.esa.int/data. To reduce the effect of noise in the GRACE monthly solutions and to make the data more comparable to our altimetry results, we applied a three-month moving average to the GRACE time series. We also compare our data to time series of cumulated surface mass balance anomalies anomaly (SMBA) from RACMO2.3p2 (SMB, van Wessem et al., 2018). Similar to the firn model, the SMB contains seasonal and interannual variations due to surface processes . However, it assumes an equilibrium over the modeled period and, hence, does (van Wessem et al., 2018). To obtain these anomalies, the gridded SMB rates have been reduced by a mean rate and integrated over time. Similar to the IMAU firn model, these SMBAs contain seasonal and interannual variations due to surface processes but do not include long-term changes over the full modeled period (1979-2016). The different time series show the good agreement of the techniques in resolving interannual variations. For example for the basin of Totten Glacier (C'-D in Fig. 12), all techniques observe a negative mass anomaly in early 2008, followed by a significant mass gain in 2009. 2009 as previously reported by Velicogna et al. (2014) and Li et al. (2016). Between 03/2008 and 10/2009, we obtain a mass difference of 116.6±27.0 Gt from altimetry, 109.4 Gt from SMB SMBA and 113.4 Gt from GRACE. The high agreement with the SMB indicates that this mass gain is caused by snow accumulation. In most of the basins, we observe SMBA indicates that this mass gain at Totten is caused by snow accumulation. In most of the basins, we observe a similar high agreement in the short-term variations. A good example for the different components of the total mass change signal is a total mass change signal which is constituted from components of SMBA and ice dynamics is the Getz and Abbot region (F-G) in West Antarctica. While all techniques observe a significant mass loss between 2009 and 2011, the SMB does not contain a long term trend, as observed by altimetry and GRACE. In some regions, however, there are also significant discrepancies between the different data sets . The poor sampling of SMBA does not contain the decadal trend, as observed by altimetry and GRACE. In some regions, there are also significant discrepancies between the northernmost APIS data sets of satellite atlimetry and GRACE. Inadequate sampling by radar altimetry (such as in the northern tip of the Antarctic Peninsula (I-I") by altimetry is a good example for the limitations of this techniquewhere steep regional topography and small outlet glacier size limits the recovery), leakage in the GRACE estimate between different sectors and uncertainties in the individual measurements and in the geophysical corrections might cause these differences. In George V Land (D-D'), the agreement during the GRACE period is reasonable, while the mass gain, indicated by the SMB SMBA in the early 1990s is not revealed by the altimetry time series.

Over the last 25 years our data indicate a clearly negative mass balance of -2068±377 Gt for the AIS (Fig. 11a). This is mainly a result of the mass loss in the WAIS over the last decade. In contrast, the EAIS has been very stable over our observational record (120±121 Gt between 1992 and 2017). The time series of the APIS contains large uncertainties due to many unobserved cells. Mass change rates for selected regions, obtained from the differences over a specific time interval, and their respective uncertainties are given in Tab. 2. We calculated separate trends for the area north of 72°S, which is covered by all satellites, the area north of 81.5°S, which is covered since ERS-1 and for the total area, which is (except the covered since CryoSat-2, except for its 500 km diameter polar gap) covered since CryoSat-2. The observed area shows that polar gap. 96.4% of the cells , classified as ice sheet north of 81.5°S , are successfully covered by observations of ERS-1. Cells without successful observation occur mostly at the APIS, where only 61% is covered with data.

From the overall mass loss of -2068±377 Gt for the AIS (<81.5°S over 1992-2017) we obtain an average long-term rate of -84.7±15.5 Gt/yr. This rate agrees within error bars but is considerably smaller than the results of Shepherd et al. (2018) of -109±56 Gt/yr. Part of this disagreement might be attributed to differences in the estimates for the Antarctic Peninsula where retrieving reliable radar altimetry estimates is non-trivial. However, the extended material in Shepherd et al. (2018) shows that there are still some discrepancies between the different techniques to determine the AIS mass balance. For the time interval 2003-2010 (Extended Data Table 4 in Shepherd et al., 2018) the Input-Output method obtains a rate of -201±82 Gt/yr for the AIS, while the mass balance rates, aggregated from satellite gravimetry (-76±20 Gt/yr) and from altimetry (-43±21 Gt/yr) agree much better with our result for the AIS (<81.5°S) between 2003 and 2010 of -64.7±24.9-65±25 Gt/yr.

Table 2. Mass change rates for different regions of the Antarctic Ice Sheet and different time intervals. The sizes of the total and observed area refer to all cells classified as ice sheet in the respective region (and, if stated, limited by the given latitude).

region	area $[10^3 \mathrm{km}^2]$		dM/dt $[\mathrm{Gt/yr}]$				
	total	observed	1978-2017	1992-2017	1978-1992	1992-2010	2010-2017
AIS	11892	11630	-	-	-	-	-117.5±25.5
EAIS	9620	9413	-	-	-	-	1.6±13.1
WAIS	2038	2008	-	-	-	-	-114.5±19.9
APIS	232	208	-	-	-	-	-4.5±8.7
AIS (<81.5°S)	9391	9053	-	-84.7±15.5	-	-58.6±20.3	-137.0±24.9
EAIS (<81.5°S)	7764	7555	-	4.9±5.0	-	8.0±6.2	2.4±12.4
WAIS (<81.5°S)	1394	1358	-	-91.7±10.3	-	-69.4±13.1	-134.9±19.6
APIS (<81.5°S)	232	142	-	2.1±8.9	-	2.8±12.3	-4.5±8.7
EAIS (<72°S)	2779	2274	1.5±5.8	-3.4±4.0	12.1±17.4	0.0±4.9	-8.4±10.1

For the APIS (<72°S), the very sparse observations of Seasat and Geosat did not allow calculate a reliable trend.

6 Discussion

6.1 Multi-mission SEC time seriesSurface elevation changes

The single-mission time series , obtained in Sect. 3.2, contain satellite-specific calibration biases as well as offsets due to the specific sampling characteristics of different sensor types. In order to form a consistent SEC time series, these biases needed to be determined and corrected. A comparison with in situ data showed that there are no significant offsets between elevation changes from our multi-mission altimetry data and the validation datasets. This comparison, however, could only validate our data in the interval 2001-2016. A quality control for the whole time span was performed by a comparison with a firn model. The correlation of the detrended data sets shows that especially for regions where the interannual variation is large (compared to the measurement noise of the altimeters) both time series agree very well. This comparison even provided independent estimates for the error of the early missions. The average differences between the detrended time series of the FDM and the SEC show that the observations of Geosat and even of Seasat agree with the model results within a few decimeters. For Combining all the single missions consistently, our SEC time series allow to analyze the long-term changes over the full time period of satellite altimetry observations. For 79% of the area of the AIS, this means a time span of 25 years. Over 25% of the ice sheet, largely in the coastal regions of East Antarctica, the time series can be extended back 40 years. Such long-term trends are significantly less affected by short-term variations in snowfall than a trend from a single mission. Furthermore, the period of observation of a single mission is short compared to climatic oscillations as reported e.g. by Mémin et al. (2015). Our extended time series helps to separate elevation change due to climate variations from potentially accelerating volume losses. Also Seasat and Geosat provide important information here. Due to the stability criteria in the calibration, we do not expect significant new insights on the East Antarctic plateau (even as regional variation still may be discernible as we used an ice-sheet-wide average in calibration). However, in the coastal regions of East Antarctica, with SECs of up to several meters w.r.t 2010 (see Fig. 6), this means that also the older data can be used to calculate elevation change rates with an accuracy better than a centimeter per year (see Fig.S7aalso the older data can contribute significant information to study elevation changes in a long-term context of 40 years (cf. the rates in Fig. 9 and their uncertainties in Fig. S9). Unfortunately, in coastal DML west of the ice divide A', the data of Seasat and Geosat are very noisy . This due to the mountain ranges just north of 72°S , which lead to many losses of lock of the measurements all the in these regions. They lead to many signal losses along the way across this part of the ice sheet. The same applies to the measurements at the APIS.

6.2 Surface elevation changes

The mean rates of elevation change in Fig. 9 show the regions which experience a significant thinning (Amundsen Sea Embayment, Totten Glacier) or thickening (Kamb Ice Stream) which was already reported by previous publications (e.g. Wingham et al., 2006b; Flament and Rémy, 2012; Helm et al., 2014; Zwally et al., 2015). By combining all the single missions consistently we analyze long-term changes over the full time period covered. For 79% of the area of the AIS, this means a time span of 25 years. For 25%, mainly the coastal regions of East Antarctica, even 40 years are covered. We assume that these long-term trends are significantly less affected by short-term variations in snowfall than a trend from a single mission.

The benefits of a seamless combination of the time series are demonstrated in Fig. 9. The time intervals for the elevation changes are independent of the observational period of a single mission. This is necessary to analyze processes which occurred close to the transition between different missions. A good example of the advantage of such long time series are the elevation changes caused by the accumulation events in DML. Figure 10c clearly shows the changes in elevation, caused by the strong snowfall events in 2009 and 2011. The mission lifetime of ICESat ended in 10/2009, CryoSat-2 provided the first measurements in 07/2010. Only Envisat covered both events but here, the orbit was shifted in 10/2010, resulting in different repeat track cells covered before and after the orbit shift. We merged all these missions as described in Sect. 3.3, which allows us to analyze the full time series. Comparing the elevation change from altimetry e. g. at point A in Fig.10c changes from altimetry with those in the FDM serves as a cross-validation of both data sets. For example at point A in Fig.10c our SEC time series observes a change of 0.55±0.50 m with the change modeled using the FDM (0.48 between 2008 and 2012) is a good example of successfully cross-validating these two data setswhile the FDM models a very similar elevation gain of 0.48 m for this period. Figure 8 shows the degree of agreement over the entire AIS.

As these elevation change rates alone do not contain any information on their origin, additional data are needed for improved process understanding. Figure 14 shows SEC rates for the interval 2002-2016 (March-September respectively) from altimetry and the FDM and respective IMAU-FDM and corresponding rates of ice mass changes from GRACE. These maps show that the elevation gains in DML and Enderby Land agree very well with the firn model, which implies that increased snow accumulation during this period is responsible for the thickening. For Princess Elizabeth Land (C-C'), the negative rates agree as well, implying that the thinning here can be related to lower than normal snow accumulation. In contrast, the strong thinning along the Amundsen Sea Embayment (G-H) or the thickening of Kamb Ice Stream (E'-F) is not present in the FDM results but does show up in the GRACE data. Due to the higher densities of the involved material, ice dynamic processes show up are even more pronounced in the map of mass changes, compared to the maps of elevation changes.

The inland propagation of dynamic thinning of the glaciers of the Amundsen Sea Embayment over the last decades has been described by Konrad et al. (2016). A recent onset of significant mass losses has also been reported for the adjacent glaciers

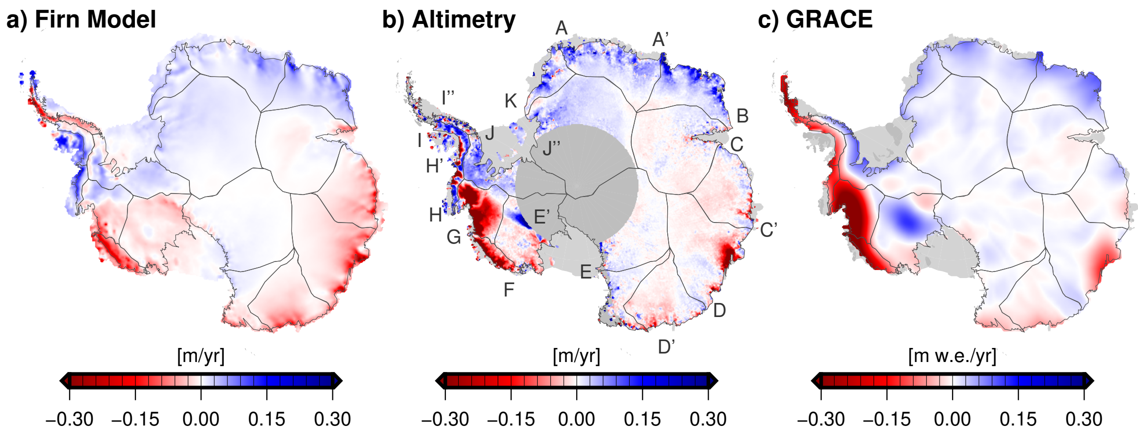

Figure 14. Mean rates for the time interval 2002-2016 of elevation changes from IMAU-FDM **(a)**, from the multi-mission SEC grids **(b)** and of the mass changes from GRACE **(c)**.

along the Bellingshausen Sea (H-I, Wouters et al., 2015) and in the Getz and Abbot region (F-G, Chuter et al., 2017). Fig. 9i reveals that the largest losses along the coast of the WAIS occurred between 2007 and 2012. The period 2012-2017 (Fig. 9i) shows that only a part of these large rates is persistent, indicating . While the ice discharge of the Getz and Abbot region even increased by 6% between 2008 and 2015 (Gardner et al., 2018), the deceleration of the elevation change after 2012 indicates that also interannual variations in SMB have to be considered here (see also Chuter et al., 2017). The FDM-derived rate in Fig. 14a confirms the role of the surface mass balance in this region.

6.2 Ice sheet mass time series

The individual basin time series for these regions time series for individual basins of the WAIS (in Fig. 12) allow us to analyze the increasing losses at a monthly resolution. They show that in In 2004, the thinning of the Getz and Abbot region accelerated and experienced a further acceleration after 2007. After a small positive mass anomaly in late 2005, which relates to a similar event in the SMB SMBA time series, the overall mass losses in the Amundsen Sea Embayment accelerated. The Bellingshausen Sea basin was relatively stable until 2009, but started to lose significant amounts of mass after that time, as reported by Wouters et al. (2015). Since this study2016, however, we observe that the basins at the western part of the Peninsula (H-I) regained mass. The comparison with SMB SMBA reveals that this can be explained by a positive snowfall anomaly in this area in 2016. The shape and orientation of the Peninsula makes GRACE observations challenging with respect to leakage and GRACE error effects (Horwath and Dietrich, 2009). Nevertheless, the results of the satellite gravity mission confirm this mass anomaly.

The comparison of the ice sheet wide mass time series between altimetry and GRACE in Fig. 11 reveals that for the WAIS, both datasets agree very well, while for the APIS and the EAIS, significant differences are found. The percentage of observed area of the APIS (gray area in the background of Fig. 11d) indicates that before 2010 a significant part of the area remained unobserved. Here, conventional RA measurements very often failed due to the rugged terrain. Even for ICESat, the large across track distances and the dependence on cloud-free conditions make measurements very sparse here. With the weather independent, dense and small footprint measurements of CryoSat-2 in SARIn mode, up to 80% of the area are covered by observations. Compared to GRACE, however, we observe a significantly weaker mass loss signal. Thomas et al. (2008) pointed out that RA fails to sample especially the large elevation changes in narrow valleys of outlet glaciers. This leads to an overall underestimation of the signal by altimetric observations. Even for ICESat this is true in this case, as cloudy conditions are not unusual in this region. But even when enough valid measurements would have been availablewhen enough valid measurements in a reasonable spatial sampling would have been available (as in the case of ICESat or CryoSat-2), the fit of a planar surface over a diameter of $2\,\mathrm{km}$ would have been very challenging in the initial repeat altimetry processing here. Our approach is designed to provide valid observations over the majority of the AIS. Under the challenging conditions of the APIS, modifications such as a smaller diameter or more complex parametrization of the surface would surely help to improve the results. Furthermore, we did not calculate a SEC for cells that are further away than a beam-limited radar footprint from valid measurements. In order to interpolate or even extrapolate the results to unobserved cells, advanced gridding methods such as kriging, especially with the help of additional data sets (Hurkmans et al., 2012), would be advisable. In contrast, here we concentrate on the observed cells only.

For the EAIS (Fig. 11b) we see significant differences between the time series of mass changes from altimetry and from GRACE. For the time interval 2002 to 2016 (see Sect. F.3), the mean rate from altimetry (9.6±6.9 $\mathrm{Gt/yr}$) is mainly dominated by the accumulation events in 2009 and 2011. In contrast, the GRACE data imply an average mass gain of 42.1 $\mathrm{Gt/yr}$ over this time interval. Especially after 2011, the differences become very prominent in the time series. The respective mass changes for the individual basins (Fig. 12) reveal that this difference in the signals can be attributed to DML and Enderby Land. This might be a sign for dynamic thickening. Here, all elevation changes have been converted to mass using the density of surface firn. If a part of the positive elevation changes in this region indeed would be caused by ice dynamics, this would lead to an underestimation of mass gains from altimetrycompared to gravimetric measurements. The results of the Bayesian combined approach of Martín-Español et al. (2017) also suggest a small dynamic thickening in this region. Rignot et al. (2008) observed no significant mass changes in this region between 1992 and 2006 using the input-output-method. Gardner et al. (2018) compared present day ice flow velocities to measurements from 2008. They obtain a slightly reduced ice discharge in DML (which would support the hypothesis of a dynamic thickening), while they observe a small increase in discharge for Enderby Land. Part of this misfit might also be explained by remaining processing issues in the GRACE processing (e.g. the GIA correction). Hence, we conclude that further workis needed to identify the origin of this discrepancythe discrepancy with the GRACE results could be also due to uncertainties in the geophysical corrections applied to the GRACE data, such as the effects of glacial isostatic adjustment. More work, similar to the Ice Sheet Mass Balance Inter-comparison Exercises (Shepherd et al., 2018) or the combination of different types of observations as in Martín-Español et al. (2016), could help identify the reason leading to the disagreement.

7 Conclusions

In this paper we presented an approach to combine different satellite altimetry missions, observation modes and techniques. The reprocessing of the conventional pulse limited radar altimetry ensures that two fundamental steps in processing of radar ice altimetry, the waveform retracking and the slope correction, are performed consistently. Furthermore, we showed that the advanced methods , used in this processing, improved the precision by more than methods used here improved the overall precision by 50% , compared to the widely used standard products. The validation with in situ over the standard data sets available from ESA and NASA. The validation with in situ and airborne measurements and the comparison with the IMAU-FDM shows that inter-mission offsets have been successfully corrected and that the uncertainty estimates for our resulting monthly multi-mission SEC grids are realistic.

We analyzed the resulting time series and found that they provide detailed insight in the evolution of the surface elevation of the Antarctic Ice Sheet. From the combined SEC time series we calculated the long-term surface elevation change over the last 25 years. Due to Seasat and Geosat , observations in the coastal EAIS date back until 1978, covering four decades. Observations from the Seasat and Geosat missions extend the time series in the coastal regions of East Antarctica back to 1978. The unique data show that large parts of the East Antarctic plateau are very close to equilibrium, while changes over shorter time intervals identify interannual variations, which cannot be identified in long-term trends and are mostly associated with snowfall anomalies.

The monthly mass time series show that the AIS (excluding the polar gap within 81.5°S) lost an average amount of mass of -84.7±15.5 $\mathrm{Gt/yr}$ between 1992 and 2017. These losses accelerated in several regions and, hence, for 2010-2017 we obtain -137.0±24.9 $\mathrm{Gt/yr}$ for the same area. The comparison of the altimetry-derived mass changes, integrated over different basins and regions of the ice sheet, with SMB SMBA and GRACE shows high consistency of the different techniques. A correlation coefficient between the mass anomalies from altimetry and from GRACE of 0.96 (for the time interval 2002-2016, see Tab. S4) indicates the excellent agreement of the observed interannual variations. The respective correlation with the SMB anomalies correlation with the SMBA (0.60 for 1992-2016) is comparatively lower but still indicates a high agreement. In the APIS, differences between the mass time series of the different techniques arise mainly due to the poor spatial sampling of the altimetry data, while for the EAIS, the remaining discrepancies to mass time series from GRACE might be explained by the density mask used or uncertainties in the GRACE processing. These remaining issues and open questions should be addressed in future work in order to further reduce the uncertainty of the estimates of the mass balance of the AIS. The recently launched laser altimeter ICESat-2 promises a new milestone in ice sheet altimetry. We believe that our multi-mission combination approach can provide an important tool to combine the extremely high resolution of this mission with the long time period, covered by the previous missionsfor including the extremely high resolution of this mission into the long-time observations of satellite altimetry spanning the past few decades.

Author contributions. L. Schröder designed the study and developed the PLRA reprocessing, the repeat altimetry processing and the time series generation. V. Helm supplied the reprocessed CryoSat-2 SARIn data. Stefan Ligtenberg and Michiel van den Broeke provided the RACMO and IMAU-FDM models. All authors discussed the results and contributed to the writing and editing of the manuscript.

Acknowledgements. This work is supported by the Deutsche Bundesstiftung Umwelt (DBU, German Federal Environmental Foundation). We thank the European Space Agency, the National Snow and Ice Data Center and the NASA Goddard Space Flight Center for providing the altimetry data products. Especially we would like to thank Jairo Santana for his support to access the GSFC data. We are very grateful for the comments from the anonymous referees, A.Shepherd and the editor E.Berthier, which significantly helped to improve and clarify the manuscript. We acknowledge support by the Open Access Publication Funds of the SLUB/TU Dresden.

References

Arthern, R., Wingham, D., and Ridout, A.: Controls on ERS altimeter measurements over ice sheets: Footprint-scale topography, backscatter fluctuations, and the dependence of microwave penetration depth on satellite orientation, Journal of Geophysical Research – Atmospheres, 106, 33 471–33 484, 2001.

Baarda, W.: A testing procedure for use in geodetic networks, Netherlands Geodetic Commission, 1968.

Bamber, J.: Ice Sheet Altimeter Processing Scheme, Int. J. Remote Sensing, 14, 925–938, 1994.

Bamber, J., Gomez-Dans, J., and Griggs, J.: A new 1 km digital elevation model of the Antarctic derived from combined satellite radar and laser data – Part 1: Data and methods, The Cryosphere, 3, 101–111, https://doi.org/10.5194/tc-3-101-2009, 2009.

Boening, C., Lebsock, M., Landerer, F., and Stephens, G.: Snowfall-driven mass change on the East Antarctic ice sheet, Geophys. Res. Lett., 39, L21 501, https://doi.org/10.1029/2012GL053316, 2012.

Brenner, A., Bindschadler, R., Zwally, H., and Thomas, R.: Slope-induced errors in radar altimetry over continental ice sheets, J. Geophys. Res., 88, 1617–1623, https://doi.org/10.1029/JC088iC03p01617, 1983.

Brenner, A., DiMarzio, J., and Zwally, H.: Precision and Accuracy of Satellite Radar and Laser Altimeter Data Over the Continental Ice Sheets, IEEE Trans. Geosci. Remote Sens., 45, 321–331, https://doi.org/10.1109/TGRS.2006.887172, 2007.

Brockley, D., Baker, S., Femenias, P., Martinez, B., Massmann, F.-H., Otten, M., Paul, F., Picard, B., Prandi, P., Roca, M., Rudenko, S., Scharroo, R., and Visser, P.: REAPER: Reprocessing 12 Years of ERS-1 and ERS-2 Altimeters and Microwave Radiometer Data, IEEE Trans. Geosci. Remote Sens., 55, 5506–5514, https://doi.org/10.1109/TGRS.2017.2709343, 2017.

Brunt, K., Hawley, R., Lutz, E., Studinger, M., Sonntag, J., Hofton, M., Andrews, L., and Neumann, T.: Assessment of NASA airborne laser altimetry data using ground-based GPS data near Summit Station, Greenland, The Cryosphere, 11, 681–692, https://doi.org/10.5194/tc-11-681-2017, 2017.

Brunt, K. M., Neumann, T. A., and Larsen, C. F.: Assessment of altimetry using ground-based GPS data from the 88S Traverse, Antarctica, in support of ICESat-2, The Cryosphere Discussions, 2018, 1–21, https://doi.org/10.5194/tc-2018-160, https://www.the-cryosphere-discuss.net/tc-2018-160/, 2018.

Chuter, S., Martín-Español, A., Wouters, B., and Bamber, J.: Mass balance reassessment of glaciers draining into the Abbot and Getz Ice Shelves of West Antarctica: Getz and Abbot Mass Balance Reassessment, Geophys. Res. Lett., 44, 7328–7337, https://doi.org/10.1002/2017GL073087, 2017.

Davis, C.: A Combined Surface/volume Scattering Retracking Algorithm for Ice Sheet Satellite Altimetry, in: Geoscience and Remote Sensing Symposium, 1992. IGARSS ’92. International, vol. 2, pp. 969–971, https://doi.org/10.1109/IGARSS.1992.578311, 1992.

Davis, C.: A robust threshold retracking algorithm for measuring ice-sheet surface elevation change from satellite radar altimeters, Geoscience and Remote Sensing, IEEE Transactions on, 35, 974–979, https://doi.org/10.1109/36.602540, 1997.

Davis, C. and Ferguson, A.: Elevation change of the Antarctic ice sheet, 1995-2000, from ERS-2 satellite radar altimetry, IEEE Trans. Geosci. Remote Sens., 42, 2437–2445, https://doi.org/10.1109/TGRS.2004.836789, 2004.

Flament, T. and Rémy, F.: Dynamic thinning of Antarctic glaciers from along-track repeat radar altimetry, J. Glac., 58, 830–840, 2012.

Frappart, F., Legrésy, B., Niño, F., Blarel, F., Fuller, N., Fleury, S., Birol, F., and Calmant, S.: An ERS-2 altimetry reprocessing compatible with ENVISAT for long-term land and ice sheets studies, Remote Sens. Environ., 184, 558–581, https://doi.org/10.1016/j.rse.2016.07.037, 2016.

Fricker, H. and Padman, L.: Thirty years of elevation change on Antarctic Peninsula ice shelves from multimission satellite radar altimetry, J. Geophys. Res., 117, https://doi.org/10.1029/2011JC007126, 2012.

Gardner, A., Moholdt, G., Scambos, T., Fahnstock, M., Ligtenberg, S., van den Broeke, M., and Nilsson, J.: Increased West Antarctic and unchanged East Antarctic ice discharge over the last 7 years, The Cryosphere, 12, 521–547, https://doi.org/10.5194/tc-12-521-2018, 2018.

Groh, A. and Horwath, M.: The method of tailored sensitivity kernels for GRACE mass change estimates, Geophys. Res. Abstr., 18, EGU2016–12 065, 2016.

Groh, A., Ewert, H., Scheinert, M., Fritsche, M., Rülke, A., Richter, A., Rosenau, R., and Dietrich, R.: An Investigation of Glacial Isostatic Adjustment over the Amundsen Sea sector, West Antarctica, Global Planet. Change, 98–99, 45–53, https://doi.org/10.1016/j.gloplacha.2012.08.001, 2012.

Helm, V., Humbert, A., and Miller, H.: Elevation and elevation change of Greenland and Antarctica derived from CryoSat-2, The Cryosphere, 8, 1539–1559, https://doi.org/10.5194/tc-8-1539-2014, 2014.

Hogg, A., Shepherd, A., Cornford, S., Briggs, K., Gourmelen, N., Graham, J., Joughin, I., Mouginot, J., Nagler, T., Payne, A., Rignot, E., and Wuite, J.: Increased ice flow in Western Palmer Land linked to ocean melting, Geophys. Res. Lett., 44, 4159–4167, https://doi.org/10.1002/2016GL072110, 2017.

Horwath, M. and Dietrich, R.: Signal and error in mass change inferences from GRACE: the case of Antarctica, Geophys. J. Int., 177, 849–864, https://doi.org/10.1111/j.1365-246X.2009.04139.x, 2009.

Horwath, M., Legrésy, B., Rémy, F., Blarel, F., and Lemoine, J.-M.: Consistent patterns of Antarctic ice sheet interannual variations from ENVISAT radar altimetry and GRACE satellite gravimetry, Geophys. J. Int., 189, 863–876, https://doi.org/10.1111/j.1365-246X.2012.05401.x, 2012.

Hurkmans, R., Bamber, J., Sørensen, L., Joughin, I., Davis, C., and Krabill, W.: Spatiotemporal interpolation of elevation changes derived from satellite altimetry for Jakobshavn Isbræ, Greenland, J. Geophys. Res., 117, https://doi.org/10.1029/2011JF002072, 2012.

Ivins, E., James, T., Wahr, J., Schrama, E., Landerer, F., and Simon, K.: Antarctic contribution to sea level rise observed by GRACE with improved GIA correction, J. Geophys. Res. Solid Earth, 118, 3126–3141, https://doi.org/10.1002/jgrb.50208, 2013.

Joughin, I., Shean, D., Smith, B., and Dutrieux, P.: Grounding line variability and subglacial lake drainage on Pine Island Glacier, Antarctica, Geophys. Res. Lett., 43, 9093–9102, https://doi.org/10.1002/2016GL070259, 2016.

Kallenberg, B., Tregoning, P., Hoffmann, J., Hawkins, R., Purcell, A., and Allgeyer, S.: A new approach to estimate ice dynamic rates using satellite observations in East Antarctica, The Cryosphere, 11, 1235–1245, https://doi.org/10.5194/tc-11-1235-2017, 2017.

Khvorostovsky, K.: Merging and Analysis of Elevation Time Series Over Greenland Ice Sheet From Satellite Radar Altimetry, IEEE Trans. Geosci. Remote Sens., 50, 23–36, https://doi.org/10.1109/TGRS.2011.2160071, 2012.

Konrad, H., Gilbert, L., Cornford, S., Payne, A., Hogg, A., Muir, A., and Shepherd, A.: Uneven onset and pace of ice-dynamical imbalance in the Amundsen Sea Embayment, West Antarctica, Geophys. Res. Lett., https://doi.org/10.1002/2016GL070733, 2016.

Lacroix, P., Dechambre, M., Legrésy, B., Blarel, F., and Rémy, F.: On the use of the dual-frequency ENVISAT altimeter to determine snowpack properties of the Antarctic ice sheet, Remote Sens. Environ., 112, 1712–1729, https://doi.org/10.1016/j.rse.2007.08.022, 2008.

Legrésy, B. and Rémy, F.: Altimetric observations of surface characteristics of the Antarctic ice sheet, J. Glac., 43, 265–276, 1997.

Legrésy, B., Rémy, F., and Schaeffer, P.: Different ERS altimeter measurements between ascending and descending tracks caused by wind induced features over ice sheets, Geophys. Res. Lett., 26, 2231–2234, https://doi.org/10.1029/1999GL900531, 1999.

Legrésy, B., Papa, F., Rémy, F., Vinay, G., van den Bosch, M., and Zanife, O.-Z.: ENVISAT radar altimeter measurements over continental surfaces and ice caps using the ICE-2 retracking algorithm, Remote Sens. Environ., 85, 150–163, https://doi.org/10.1016/j.rse.2004.11.018, 2005.

Legrésy, B., Rémy, F., and Blarel, F.: Along track repeat altimetry for ice sheets and continental surface studies, in: Proc. Symposium on 15 years of Progress in Radar Altimetry, Venice, Italy, 13–18 March 2006, European Space Agency Publication Division, Noordwijk, The Netherlands, eSA-SP No. 614, paper No. 181, 2006.

Lenaerts, J., van Meijgaard, E., van den Broeke, M., Ligtenberg, S., Horwath, M., and Isaksson, E.: Recent snowfall anomalies in Dronning Maud Land, East Antarctica, in a historical and future climate perspective, Geophys. Res. Lett., 40, 2684–2688, https://doi.org/10.1002/grl.50559, 2013.

Li, X., Rignot, E., Morlighem, M., Mouginot, J., and Scheuchl, B.: Grounding line retreat of Totten Glacier, East Antarctica, 1996 to 2013, Geophys. Res. Lett., 42, 8049–8056, https://doi.org/10.1002/2015GL065701, 2015.

Li, X., Rignot, E., Mouginot, J., and Scheuchl, B.: Ice flow dynamics and mass loss of Totten Glacier, East Antarctica, from 1989 to 2015, Geophys. Res. Lett., 43, 6366–6373, https://doi.org/10.1002/2016GL069173, 2016.

Li, Y. and Davis, C.: Decadal Mass Balance of the Greenland and Antarctic Ice Sheets from High Resolution Elevation Change Analysis of ERS-2 and Envisat Radar Altimetry Measurements, in: IEEE International Geoscience & Remote Sensing Symposium, IGARSS 2008, July 8-11, 2008, Boston, Massachusetts, USA, Proceedings, pp. 339–342, IEEE, https://doi.org/10.1109/IGARSS.2008.4779727, 2008.

Ligtenberg, S., Helsen, M., and van den Broeke, M.: An improved semi-empirical model for the densification of Antarctic firn, The Cryosphere, 5, 809–819, https://doi.org/10.5194/tc-5-809-2011, 2011.

Martin, T., Zwally, H., Brenner, A., and Bindschadler, R.: Analysis and retracking of continental ice sheet radar altimeter waveforms, J. Geophys. Res., 88, 1608, https://doi.org/10.1029/JC088iC03p01608, 1983.

Martín-Español, A., Zammit-Mangion, A., Clarke, P., Flament, T., Helm, V., King, M., Luthcke, S., Petrie, E., Rémy, F., Schön, N., Wouters, B., and Bamber, J.: Spatial and temporal Antarctic Ice Sheet mass trends, glacio-isostatic adjustment and surface processes from a joint inversion of satellite altimeter, gravity and GPS data, J. Geophys. Res. Earth Surf., 121, 182–200, https://doi.org/10.1002/2015JF003550, 2016.

Martín-Español, A., Bamber, J., and Zammit-Mangion, A.: Constraining the mass balance of East Antarctica, Geophys. Res. Lett., 44, https://doi.org/10.1002/2017GL072937, 2017.

McMillan, M., Shepherd, A., Sundal, A., Briggs, K., Muir, A., Ridout, A., Hogg, A., and Wingham, D.: Increased ice losses from Antarctica detected by CryoSat-2, Geophys. Res. Lett., 41, 3899–3905, https://doi.org/10.1002/2014GL060111, 2014.

McMillan, M., Leeson, A., Shepherd, A., Briggs, K., Armitage, T., Hogg, A., Kuipers Munneke, P., van den Broeke, M., Noël, B., van de Berg, W., Ligtenberg, S., Horwath, M., Groh, A., Muir, A., and Gilbert, L.: A high-resolution record of Greenland mass balance, Geophys. Res. Lett., 43, 7002–7010, https://doi.org/10.1002/2016GL069666, 2016.

Mémin, A., Flament, T., Alizier, B., Watson, C., and Rémy, F.: Interannual variation of the Antarctic Ice Sheet from a combined analysis of satellite gravimetry and altimetry data, Earth Planet. Sci. Lett., 422, 150–156, https://doi.org/10.1016/j.epsl.2015.03.045, 2015.

Michel, A., Flament, T., and Rémy, F.: Study of the Penetration Bias of ENVISAT Altimeter Observations over Antarctica in Comparison to ICESat Observations, Remote Sensing, 6, 9412–9434, https://doi.org/10.3390/rs6109412, 2014.

Miles, B., Stokes, C., and Jamieson, S.: Velocity increases at Cook Glacier, East Antarctica, linked to ice shelf loss and a subglacial flood event, The Cryosphere, 12, 3123–3136, https://doi.org/10.5194/tc-12-3123-2018, 2018.

Mouginot, J., Rignot, E., and Scheuchl, B.: Sustained increase in ice discharge from the Amundsen Sea Embayment, West Antarctica, from 1973 to 2013, Geophys. Res. Lett., 41, 1576–1584, https://doi.org/10.1002/2013GL059069, 2014.

Nilsson, J., Vallelonga, P., Simonsen, S., Sørensen, L., Forsberg, R., Dahl-Jensen, D., Hirabayashi, M., Goto-Azuma, K., Hvidberg, C., Kjaer, H., and Satow, K.: Greenland 2012 melt event effects on CryoSat-2 radar altimetry, Geophys. Res. Lett., 42, 3919–3926, https://doi.org/10.1002/2015GL063296, 2015.

Nilsson, J., Gardner, A., Sandberg Sørensen, L., and Forsberg, R.: Improved retrieval of land ice topography from CryoSat-2 data and its impact for volume-change estimation of the Greenland Ice Sheet, The Cryosphere, 10, 2953–2969, https://doi.org/10.5194/tc-10-2953-2016, 2016.

Paolo, F., Fricker, H., and Padman, L.: Constructing improved decadal records of Antarctic ice shelf height change from multiple satellite radar altimeters, Remote Sens. Environ., 177, 192–205, https://doi.org/10.1016/j.rse.2016.01.026, 2016.

Pritchard, H., Arthern, R., Vaughan, D., and Edwards, L.: Extensive dynamic thinning on the margins of the Greenland and Antarctic ice sheets, Nature, 461, 971–975, https://doi.org/10.1038/nature08471, 2009.

Rémy, F. and Parouty, S.: Antarctic Ice Sheet and Radar Altimetry: A Review, Remote Sensing, 1, 1212–1239, https://doi.org/10.3390/rs1041212, 2009.

Richter, A., Popov, S., Dietrich, R., Lukin, V., Fritsche, M., Lipenkov, V., Matveev, A., Wendt, J., Yuskevich, A., and Masolov, V.: Observational evidence on the stability of the hydro-glaciological regime of subglacial Lake Vostok, Geophys. Res. Lett., 35, L11 502, https://doi.org/10.1029/2008GL033397, 2008.

Richter, A., Popov, S., Fritsche, M., Lukin, V., Matveev, A., Ekaykin, A., Lipenkov, V., Fedorov, D., Eberlein, L., Schröder, L., Ewert, H., Horwath, M., and Dietrich, R.: Height changes over subglacial Lake Vostok, East Antarctica: Insights from GNSS observations, J. Geophys. Res. Earth Surf., 119, 2460–2480, https://doi.org/10.1002/2014JF003228, 2014.

Rignot, E.: Changes in ice dynamics and mass balance of the Antarctic ice sheet, Phil. Trans. R. Soc. Lond. A, 364, 1637–1655, 2006.

Rignot, E., Bamber, J., van den Broeke, M., Davis, C., Li, Y., van de Berg, W., and van Meijgaard, E.: Recent Antarctic ice mass loss from radar interferometry and regional climate modelling, Nature Geosci., 1, 106–110, https://doi.org/10.1038/ngeo102, 2008.

Rignot, E., Mouginot, J., and Scheuchl, B.: Ice Flow of the Antarctic Ice Sheet, Science, 333, 1427–1430, https://doi.org/10.1126/science.1208336, 2011.

Rignot, E., Mouginot, J., Morlighem, M., Seroussi, H., and Scheuchl, B.: Widespread, rapid grounding line retreat of Pine Island, Thwaites, Smith, and Kohler glaciers, West Antarctica, from 1992 to 2011, Geophys. Res. Lett., 41, 3502–3509, https://doi.org/10.1002/2014GL060140, 2014.

Rignot, E., Mouginot, J., and Scheuchl, B.: MEaSUREs InSAR-Based Antarctica Ice Velocity Map, Version 2., Boulder, Colorado USA. NASA National Snow and Ice Data Center Distributed Active Archive Center, https://doi.org/10.5067/D7GK8F5J8M8R., [date accessed: 2017-04-24], 2017.

Roemer, S., Legrésy, B., Horwath, M., and Dietrich, R.: Refined analysis of radar altimetry data applied to the region of the subglacial Lake Vostok / Antarctica, Remote Sens. Environ., 106, 269–284, https://doi.org/10.1016/j.rse.2006.02.026, 2007.

Schröder, L., Richter, A., Fedorov, D., Eberlein, L., Brovkov, E., Popov, S., Knöfel, C., Horwath, M., Dietrich, R., Matveev, A., Scheinert, M., and Lukin, V.: Validation of satellite altimetry by kinematic GNSS in central East Antarctica, The Cryosphere, 11, 1111–1130, https://doi.org/10.5194/tc-11-1111-2017, 2017.

Scott, R., Baker, S., Birkett, C., Cudlip, W., Laxon, S., Mantripp, D., Mansley, J., Morley, J., Rapley, C., Ridley, J., Strawbridge, F., and Wingham, D.: A comparison of the performance of the ice and ocean tracking modes of the ERS-1 radar altimeter over non-ocean surfaces, Geophys. Res. Lett., 21, 553–556, https://doi.org/10.1029/94GL00178, 1994.

Shepherd, A., Ivins, E., A, G., Barletta, V., Bentley, M., Bettadpur, S., Briggs, K., Bromwich, D., Forsberg, R., Galin, N., Horwath, M., Jacobs, S., Joughin, I., King, M., Lenaerts, J., Li, J., Ligtenberg, S., Luckman, A., Luthcke, S., McMillan, M., Meister, R., Milne, G., Mouginot, J., Muir, A., Nicolas, J., Paden, J., Payne, A., Pritchard, H., Rignot, E., Rott, H., Sorensen, L., Scambos, T., Scheuchl, B., Schrama, E., Smith, B., Sundal, A., van Angelen, J., van de Berg, W., van den Broeke, M., Vaughan, D., Velicogna, I., Wahr, J., Whitehouse, P., Wingham, D., Yi, D., Young, D., and Zwally, H.: A Reconciled Estimate of Ice-Sheet Mass Balance, Science, 338, 1183–1189, https://doi.org/10.1126/science.1228102, 2012.

Shepherd, A., Ivins, E., Rignot, E., Smith, B., van den Broeke, M., Velicogna, I., Whitehouse, P., Briggs, K., Joughin, I., Krinner, G., Nowicki, S., Payne, T., Scambos, T., Schlegel, N., A, G., Agosta, C., Ahlstrøm, A., Babonis, G., Barletta, V., Blazquez, A., Bonin, J., Csatho, B., Cullather, R., Felikson, D., Fettweis, X., Forsberg, R., Gallee, H., Gardner, A., Gilbert, L., Groh, A., Gunter, B., Hanna, E., Harig, C., Helm, V., Horvath, A., Horwath, M., Khan, S., Kjeldsen, K., Konrad, H., Langen, P., Lecavalier, B., Loomis, B., Luthcke, S., McMillan, M., Melini, D., Mernild, S., Mohajerani, Y., Moore, P., Mouginot, J., Moyano, G., Muir, A., Nagler, T., Nield, G., Nilsson, J., Noel, B., Otosaka, I., Pattle, M., Peltier, W., Pie, N., Rietbroek, R., Rott, H., Sandberg-Sørensen, L., Sasgen, I., Save, H., Scheuchl, B., Schrama, E., Schröder, L., Seo, K.-W., Simonsen, S., Slater, T., Spada, G., Sutterley, T., Talpe, M., Tarasov, L., van de Berg, W., van der Wal, W., van Wessem, M., Vishwakarma, B., Wiese, D., and Wouters, B.: Mass balance of the Antarctic Ice Sheet from 1992 to 2017, Nature, 558, 219–222, https://doi.org/10.1038/s41586-018-0179-y, 2018.

Simonsen, S. and Sørensen, L.: Implications of changing scattering properties on Greenland ice sheet volume change from Cryosat-2 altimetry, Remote Sens. Environ., 190, 207–216, https://doi.org/10.1016/j.rse.2016.12.012, 2017.

Studinger, M.: IceBridge ATM L4 Surface Elevation Rate of Change, Version 1. Updated 2017., Boulder, Colorado USA. NASA National Snow and Ice Data Center Distributed Active Archive Center, https://doi.org/10.5067/BCW6CI3TXOCY, [date accessed: 2018-02-28], 2014.

Thomas, E., Hosking, J., Tuckwell, R., Warren, R., and Ludlow, E.: Twentieth century increase in snowfall in coastal West Antarctica, Geophys. Res. Lett., 42, 9387–9393, https://doi.org/10.1002/2015GL065750, 2015.

Thomas, R., Davis, C., Frederick, E., Krabill, W., Li, Y., Manizade, S., and Martin, C.: A comparison of Greenland ice-sheet volume changes derived from altimetry measurements, J. Glac., 54, 203–212, https://doi.org/10.3189/002214308784886225, 2008.

van Wessem, J., van de Berg, W., Noël, B., van Meijgaard, E., Amory, C., Birnbaum, G., Jakobs, C., Krüger, K., Lenaerts, J., Lhermitte, S., Ligtenberg, S., Medley, B., Reijmer, C., van Tricht, K., Trusel, L., van Ulft, L., Wouters, B., Wuite, J., and van den Broeke, M.: Modelling the climate and surface mass balance of polar ice sheets using RACMO2 – Part 2: Antarctica (1979–2016), The Cryosphere, 12, 1479–1498, https://doi.org/10.5194/tc-12-1479-2018, 2018.

Velicogna, I., Sutterley, T., and van den Broeke, M.: Regional acceleration in ice mass loss from Greenland and Antarctica using GRACE time-variable gravity data, Geophys. Res. Lett., 41, 8130–8137, https://doi.org/10.1002/2014GL061052, 2014.

Wingham, D., Rapley, C., and Griffiths, H.: New techniques in satellite altimeter tracking systems, in: ESA Proceedings of the 1986 International Geoscience and Remote Sensing Symposium(IGARSS'86) on Remote Sensing: Today's Solutions for Tomorrow's Information Needs,, vol. 3, pp. 1339–1344, 1986.

Wingham, D., Ridout, A., Scharroo, R., Arthern, R., and Shum, C.: Antarctic Elevation Change from 1992 to 1996, Science, 282, 456–458, https://doi.org/10.1126/science.282.5388.456, 1998.

Wingham, D., Francis, C., Baker, S., Bouzinac, C., Brockley, D., Cullen, R., Chateau-Thierry, P. d., Laxon, S., Mallow, U., Mavrocordatos, C., Phalippou, L., Ratier, G., Rey, L., Rostan, F., Viau, P., and Wallis, D.: CryoSat: A mission to determine the fluctuations in Earth's land and marine ice fields, Adv. Space Res., 37, 841–871, https://doi.org/10.1016/j.asr.2005.07.027, 2006a.

Wingham, D., Shepherd, A., Muir, A., and Marshall, G.: Mass balance of the Antarctic ice sheet, Phil. Trans. R. Soc. Lond. A, 364, 1627–1635, https://doi.org/10.1098/rsta.2006.1792, 2006b.

Wouters, B., Bamber, J., van den Broeke, M., Lenaerts, J., and Sasgen, I.: Limits in detecting acceleration of ice sheet mass loss due to climate variability, Nature Geosci., 6, 613–616, https://doi.org/10.1038/ngeo1874, 2013.

Wouters, B., Martín-Español, A., Helm, V., Flament, T., van Wessem, J., Ligtenberg, S., van den Broeke, M., and Bamber, J.: Dynamic thinning of glaciers on the Southern Antarctic Peninsula, Science, 348, 899–903, https://doi.org/10.1126/science.aaa5727, 2015.

Zwally, H., Giovinetto, M., Li, J., Cornejo, H., Beckley, M., Brenner, A., Saba, J., and Yi, D.: Mass changes of the Greenland and Antarctic ice sheets and shelves and contributions to sea-level rise: 1992-2002, J. Glac., 51, 509–527, https://doi.org/10.3189/172756505781829007, 2005.

Zwally, H., Li, J., Robbins, J., Saba, J., Yi, D., and Brenner, A.: Mass gains of the Antarctic ice sheet exceed losses, J. Glac., 61, 1019–1936, 2015.